

Template-directed biopolymerization: tape-copying Turing machines*

Ajeet K. Sharma¹ and Debashish Chowdhury¹

¹*Department of Physics, Indian Institute of Technology, Kanpur 208016, India*

(Dated: January 1, 2013)

DNA, RNA and proteins are among the most important macromolecules in a living cell. These molecules are polymerized by molecular machines. These natural nano-machines polymerize such macromolecules, adding one monomer at a time, using another linear polymer as the corresponding template. The machine utilizes input chemical energy to move along the template which also serves as a track for the movements of the machine. In the Alan Turing year 2012, it is worth pointing out that these machines are “tape-copying Turing machines”. We review the operational mechanisms of the polymerizer machines and their collective behavior from the perspective of statistical physics, emphasizing their common features in spite of the crucial differences in their biological functions. We also draw attention of the physics community to another class of modular machines that carry out a different type of template-directed polymerization. We hope this review will inspire new kinetic models for these modular machines.

* Contribution in the Alan Turing year 2012

Abbreviations	
A	Adenosine
T	Thymine
C	Cytosine
G	Guanine
U	Uracil
RNA	Ribonucleic acid
DNA	Deoxyribonucleic acid
mRNA	Messenger RNA
rRNA	Ribosomal RNA
tRNA	Transfer RNA
NTP	Nucleotide triphosphate
ATP	Adenosine triphosphate
GTP	Guanosine triphosphate
GDP	Guanosine diphosphate
dNTP	Deoxyribonucleotide triphosphate
DDRP	DNA dependent RNA polymerase
DDDP	DNA dependent DNA polymerase
RDRP	RNA dependent RNA polymerase
RDDP	RNA dependent DNA polymerase
RNAP	RNA polymerase
DNAP	DNA polymerase
dsDNA	Double stranded DNA
ssDNA	Single stranded DNA
PP_i	Pyrophosphate
TEC	Transcription elongation complex
ASEP	Asymmetric simple exclusion process
TASEP	Totally asymmetric simple exclusion process
ADP	Adenosine diphosphate
LTR	Long terminal repeats
HIV	Human immunodeficiency virus
AIDS	Acquired immunodeficiency syndrome
RNaseH	Ribonuclease H
RT	Reverse transcriptase
aa-tRNA	Aminoacyl tRNA
aa-tRNA synth	Aminoacyl tRNA synthetase
EF-Tu	Elongation factor thermo unstable
EF-G	Elongation factor G
DTD	Dwell time distribution
L or Leu	Leucine
Phe or F	Phenylalanine
UTR	Untranslated region
NRPS	Nonribosomal peptide synthetase
PKS	Polyketide synthase
FAS	Fatty acid synthase
KS	Ketosynthase
AT	Acyl transferase
ACP	Acyl carrier protein
KR	Ketoreductase
DH	Dehydratase
ER	Enoyl reductase
PCP-domain	Peptidyl carrier domain

Abbreviations	
C-domain	Condensation domain
A-domain	Adenylation domain
MT-domain	Methyltransferase domain
E-domain	Epimerisation domain
TE-domain	Thioesterase domain

Symbols	
ℓ	Covering length of a molecular machine.
$Q(i j)$	Conditional probability that, given a RNAP at site i , there is no RNAP at site j .
ρ	Number density of molecular machines on its one dimensional track.
ρ_{cov}	Coverage density of molecular machines on its one dimensional track.
J	Overall rate of RNA synthesis.
k	Replication speed.
F	Force applied on the dsDNA.
f_{dwell}	Dwell time distribution of the ribosome.
E_c	Closed finger configuration of DNAP.
E_o	Open finger configuration of DNAP.
D_n	Position of the catalytic site of DNAP, on its one dimensional track (n_{th}).
oriC	Initiation site in replication process.
terC	Termination site in replication process.
\mathcal{P}_n	Probability of reaching the RNAP at termination site($n = N$) by incorporating a correct nucleotide at position n .
$P_m(t)$	Probability of finding the TEC at m (relative position of the RNAP catalytic site with last incorporated nucleotide) at time t , having started at $m = 0$ at time $t = 0$.

I. INTRODUCTION

Biological information is chemically encoded in the sequence of the species of the monomeric subunits of a class of linear polymers that play crucial roles in sustaining and propagating “life”. Nature also designed wonderful machineries for polymerizing such macromolecules, step by step adding one monomer at each step, using another existing biopolymer as the corresponding template [1]. In this review we summarize the recent progress in understanding the common features of the structural design of these machines and stochastic kinetics of the polymerization processes.

In 1937, Alan Turing developed an abstract concept of a computing machine which was later named after him. On the occasion of the birth centenary of Alan Turing this year (2012), we emphasize the striking similarities between a Turing machine and the machines for template-directed polymerization of macromolecules of life [2].

In a cell there are three different types of macromolecules, namely, polynucleotides, polypeptides and polysaccharides, which perform wide range of important functions. The individual *monomeric residues* that form nucleic acids and proteins are *nucleotides* and *amino acids*, respectively. Both these types of macromolecules are *unbranched* polymers. De-oxyribo nucleic acid (DNA) and Ribonucleic acid (RNA) are polynucleotides whereas proteins are polypeptides. Nature uses 20 different species of amino acid subunits to make proteins; each amino acid species is denoted by three-letter symbols. In contrast, nature uses 4 different types of nucleotides, denoted by the one-letter symbols A, T, C and G, for making DNA. Similarly, 4 types of nucleotides used for making RNA are A, U, C, and G. Discovering the genetic code [3] that connects the 4-letter alphabet of the polynucleotides with the 20-letter alphabet of the polypeptides was one of the greatest puzzle-solving exercise in molecular biology of the 20th century. Messenger RNA (mRNA), ribosomal RNA (rRNA) and transfer RNA (tRNA) together form the group of “core” RNAs. It is also worth pointing out that only mRNA is translated whereas rRNA and tRNA form key components of the machinery that carries out translation.

In spite of the differences between their constituent monomers as well as in their primary, secondary and tertiary structures, nucleic acids and proteins share some common features in the birth and maturation. The main stages in the synthesis of polynucleotides by the polymerase machines are common: (a) *initiation*: Once the polymerase encounters a specific sequence on the template that acts as a chemically coded start signal, it initiates the synthesis of the product. This stage is completed when the nascent product becomes long enough to stabilize the macromolecular machine complex against dissociation from the template.

(b) *elongation*: During this stage, the nascent product gets elongated by the addition of nucleotides.

(c) *termination*: Normally, the process of synthesis is terminated, and the newly polymerized full length product molecule is released, when the polymerase encounters the *terminator* (or, stop) sequence on the template. However, we shall consider, almost exclusively, the process of *elongation*. Other common features of template-directed polymerization are as follows:

- (i) Both nucleic acids and proteins are made from a limited number of different species of monomeric building blocks.
- (ii) The sequence of the monomeric subunits to be used for synthesis are directed by the corresponding template.
- (iii) The process goes through three phases, namely, *initiation*, *elongation* and *termination*.
- (iv) During the elongation phase, the polymers are elongated, step-by-step, by successive addition of monomers, one at a time.

(v) For template-directed polymerization, the selection of the correct molecular species of subunit requires a mechanism of “molecular recognition”. However, if this mechanism is not perfect, errors can occur. The typical probability of the errors in the final product is about 1 (a) in 10^3 polymerized amino acids, in case of protein synthesis [4, 5], (b) in 10^4 polymerized nucleotides in case of mRNA synthesis [6], and (c) in 10^9 polymerized nucleotides in case of replication of DNA [7]. Purely thermodynamic discrimination of different species of nucleotide monomers cannot account for such high fidelity of polymerization. A normal living cell has mechanisms of “kinetic proofreading” and “editing” so as to detect and correct errors. A theory that explains the physical origin of dissipation in computation [8] also provides insight into the need for energy expenditure in proofreading processes during the transfer of genetic information [9, 10].

(vi) The primary product of the synthesis, namely, polynucleotide or polypeptide, often requires “processing” whereby the modified product matures into functional nucleic acid or protein, respectively.

The free energy released by each event of the phosphate ester hydrolysis, that elongates the polynucleotide by one monomer, serves as the input energy for driving the mechanical movements of the corresponding polymerase by one step on its track. Moreover, as we’ll discuss in detail later, GTP molecules are hydrolyzed during the process of polymerization of polypeptides. Therefore, the machines for template- directed polymerization are also regarded as molecular motors; these use the template itself also as the track for their translocation.

The molecular machines that polymerize polynucleotides are called *polymerase* whereas a *ribosome* polymerizes a polypeptide. The genome of both prokaryotic and eukaryotic cells consist of DNA. However, many viruses use RNA as their genetic material. For their multiplication, viruses need not only to make copies of their genetic material, but also

to manufacture the proteinous materials for constructing the capsids into which the freshly copied genomes have to be packaged. However, wide varieties of viruses do not have their own polymerases and none have their own ribosomes. Therefore, viruses exploit the machinery of their host for their own gene expression and genome replication.

A systematic and unambiguous nomenclature for polymerases is based on the nature of the template and product polynucleotides [11]: Both DNA-dependent RNA polymerase (DDRP) and DNA-dependent DNA polymerase (DDDP) use DNA as their templates; however, the former synthesizes a RNA molecule whereas the latter polymerizes a DNA. Similarly, RNA-dependent RNA polymerase (RDRP) and RNA-dependent DNA polymerase, both of which use RNA molecules as the templates, synthesize RNA and DNA molecules, respectively. The DDRP and DDDP that drive transcription and genome replication, respectively, of a cell are usually referred to as RNA polymerase (RNAP) and DNA polymerase (DNAP).

In this review we focus on the operational mechanisms of single machines engaged in template-directed polymerization in isolation as well as the collective phenomena caused by the interactions of the machines when involved simultaneously in the process.

The main quantities of interest in the context of the mechanism of a single machine are: (a) the rate of synthesis of the macromolecules, and (b) the fraction of erroneous monomers incorporated in the final product. Although most of the works initially focussed on the average rates and average error, the fluctuations in these quantities is receiving more attention in recent years.

In a living cell most often polymerases do not work in isolation. A double stranded DNA serves as the track simultaneously for several polymerases. Therefore, discovering the “traffic-rules” [12–17] for the polymerases is essential for understanding the coordination of transcription of different genes as well as that between transcription and replication. In this context, we explore the different types of possible “binary collisions” between two polymerases and the corresponding outcomes of the collisions. We also review the studies on the causes and consequences of traffic-like collective movements of many machines of the same type simultaneously on the same track in the same direction. Finally, we draw attention of the biophysics community to some modular machines that also carry out “template-directed” polymerization of a different type; quantitative modeling of these machines and their mechanisms from the perspective of physicists is desirable.

II. COMMON STRUCTURAL FEATURES OF POLYNUCLEOTIDE POLYMERASES

A polymerase is expected to have binding sites for (a) the template strand, (b) the nascent polynucleotide strand, and (c) the NTP subunits. It must have a mechanism to recognize and select the appropriate NTP directed by the template and a mechanism to catalyze the addition of the NTP thus selected to the growing polynucleotide. It would also be desirable to correct any error immediately before proceeding to the next step. A polymerase must be able to step forward by one nucleotide on its template without completely destabilizing the ternary complex consisting of the polymerase, the template and the product. Finally, it must have mechanisms for initiation and termination of the polymerization process. For several of these functions, particularly for initiation and termination, it requires assistance of other proteins.

There are several common architectural features of all polynucleotide polymerases. The shape of the polymerase has some resemblance with the “cupped right hand” of a normal human being; the three major domains of it are identified with “fingers”, “palm” and “thumb”. There are, of course, some crucial differences in the details of the architectural designs of these machines which are essential for their specific functions. The most obvious functional commonality between these machines is that these add nucleotides, the monomeric subunits of the nucleic acids, one by one following the template encoded in the sequence of the nucleotides of the template. However, in spite of the gross architectural similarities between the polymerases in prokaryotic and eukaryotic cells, there are significant differences in the primary sequences of these machines.

III. DDRP AND TRANSCRIPTION

A. Single DDRP: speed and fidelity of transcription

A common architectural feature of all DDRPs is the “main internal channel” which can accomodate a DNA/RNA hybrid that is typically 8 to 9 bp long. The NTP monomers enter through another pore-like “entry channel” while the nascent transcript emerges through the “exit channel”. The formation of the bond between the newly arrived NTP and the RNA chain takes place at a catalytically active site located at the junction of the entry pore and the main channel. In principle, during actual transcription, it may be necessary first to unwind the DNA, at least locally, to get access to the nucleotide sequence on a single-stranded DNA. Interestingly, the RNAP itself exhibits helicase

activity for this purpose. A “transcription-elongation complex” (TEC), as shown schematically in fig.1, is formed by the RNAP, the dsDNA and the nascent RNA transcript.

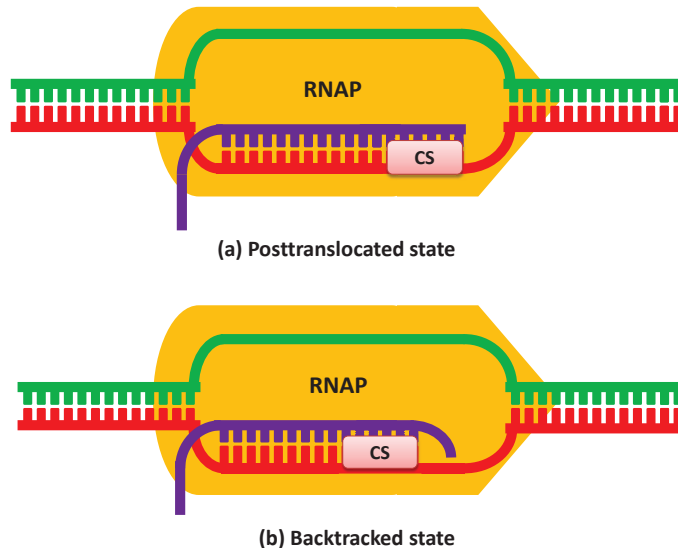


FIG. 1: Schematic representation of TEC in (a) post-translocated state (b) backtracked state

In the elongation stage, each cycle involves two main processes: polymerization and translocation. Polymerization elongates the RNA transcript by one nucleotide. During translocation, the RNAP moves forward by one nucleotide on the DNA template. The polymerase can fluctuate between two positions that are designated as “pre-translocated” and the “post-translocated” positions. In the absence of NTP, the RNAP executes an unbiased Brownian motion between these two positions. However, an incoming NTP, upon binding, rectifies the fluctuations of the RNAP thereby biasing its movement in the forward direction. Thus NTP serves as a “pawl” in this Brownian ratchet mechanism [18–24]. Yu and Oster [25] have developed a model that allow two parallel paths- one of these is based essentially on a Brownian ratchet mechanism whereas the other utilizes a power stroke. Not all kinetic models explicitly assume either the power stroke or the Brownian ratchet mechanism. Some purely kinetic models [26–28] can be interpreted in either way because these assume movements of the RNAP without explicitly explaining how these movements are caused by the energy transduction mechanism.

Single molecule studies of DDRP have provided quantitative data on the force-velocity relation for these motors. Calculation of the dwell time distribution [27, 29] of RNAP is complicated because of the varieties of paused states. A RNAP can “backtrack” on its track, i.e., reverse translocate on its template by a few steps (see fig.1). Paused states resulting from backtracking may be intrinsically different from the relatively shorter-lived paused states without backtracking [30]. The mechanisms of pausing and backtracking of RNAPs are still hotly debated [31–35]. Stochastic models have been developed for the kinetics of backtracking [36–40].

Some of these models explicitly incorporate steps for proofreading by either an isolated single RNAP [41] or by individual RNAP motors in a traffic of RNAPs [42]. In the model of nucleolytic proofreading developed by Voliotis et al. [41] the integer index n denotes the position of the last transcribed nucleotide on the template DNA. Another integer index m denotes the position of the RNAP catalytic site with respect to n . For a fixed n , $P_m(t)$ is the probability of finding the TEC at m at time t , having started at $m = 0$ at time $t = 0$. Voliotis et al.[41] defined \mathcal{P}_n as the probabilities for reaching the termination site $n = N$, having incorporated the correct nucleotide at the position n (and a similar probability for incorporating an incorrect nucleotide at n). Formulating a mathematical description, based on master equations for these probabilities, Voliotis et al.[41] derived a site-wise detailed measure of the transcriptional error.

B. Effects of RNAP-RNAP collision and RNAP traffic congestion

Two RNAPs can collide while transcribing either (i) the same gene, or (ii) two different genes. While transcribing the same gene simultaneously, the two RNAPs would move on the same DNA template strand and are co-directional.

This situation is analogous to that of two vehicles in the same lane of a highway where both the vehicles are supposed to enter and exit the traffic at the same entry and exit points on this highway. In such a co-directional collision, does the trailing polymerase get obstructed by the leading polymerase or does the leading polymerase get pushed from behind? The leading RNAP may stall either because of backtracking or because of “roadblocks” created by other DNA-binding proteins. In both these situations, the co-directional trailing RNAP can rescue the stalled leading RNAP by “pushing” it forward from behind [43, 44].

Two distinct underlying mechanisms can manifest as “pushing” by the trailing RNAP [45]- in the first, the push exerted by the trailing RNAP on the leading stalled RNAP is a “power stroke”; in the second, the leading stalled RNAP resumes transcription by thermal fluctuation just when the trailing one reaches it from behind thereby rectifying the backward movement of the leading RNAP by a “Brownian ratchet” mechanism. The elasticity of the TECs may give rise other possible outcomes of RNAP-RNAP collisions. For example, if the leading RNAP is “obstructed” by a sufficiently strong barrier, the trailing RNAP can backtrack after suffering collision with it [46].

Next we consider the more complex situation where the two interacting RNAPs transcribe two different genes. The RNAP transcribing one gene can interfere with the *initiation*, or *elongation*, or *termination* of transcription of another neighbouring gene. The plausible scenarios of such “transcriptional interference” and the corresponding outcome of the RNAP-RNAP collisions have been studied quantitatively by a kinetic model [47]. Simultaneous transcription of a gene by many DDRP motors can give rise to “traffic congestion” on the DNA track. Various aspects of this phenomenon, particularly, the effects of RNAP traffic congestion on the average rate of transcription has been investigated by an extension of the asymmetric simple exclusion process (ASEP) [26, 48, 49]. In a special case of ASEP, called totally asymmetric simple exclusion process (TASEP) particles cannot take backward step.

The kinetics of RNAP in a stochastic model [26] is shown in figure 2. The rate of transition (i.e., transition probability per unit time) from state j to the state i is denoted by ω_{ij} . In this two state model of RNAP [26] integer index “1” is assigned to a state of RNAP, where no PP_i is bound to it, while PP_i bound RNAP is represented by symbol “2”. Depending upon the different circumstances, polymerization step occurs with three different rates. If the NTP hydrolysis takes place (i) on RNAP (ii) in the solution while no PP_i is bound to it and (iii) in the solution while PP_i is bound with RNAP, then the polymerization step occurs with rate ω_{21} , ω_{11}^f and ω_{22}^f respectively. Considering that all types of polymerization reactions are reversible, then the corresponding backward transition rates are symbolized by ω_{12}^b , ω_{11}^b and ω_{22}^b , respectively. The release of PP_i ($2(i) \rightarrow 1(i)$) takes place with rate ω_{21} while its backward reaction occurs with rate ω_{12} .

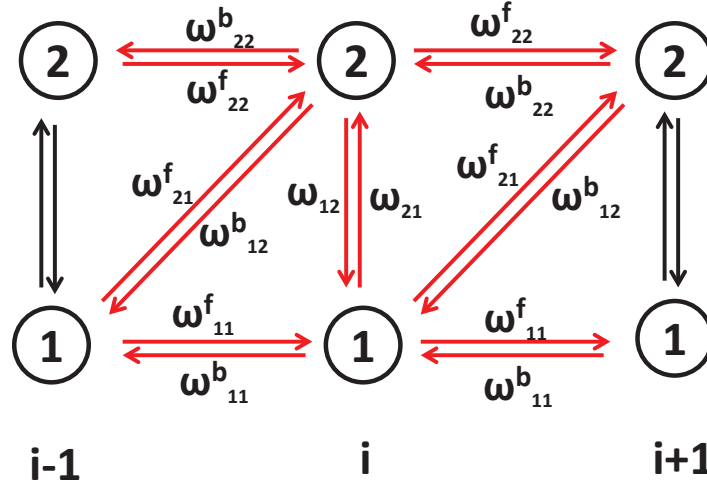


FIG. 2: Pictorial depiction of the two state model of RNAP (see the text for details).

RNAP traffic moving on the DNA track resembles an ASEP where particles are replaced by rods of the length ℓ and often referred as ℓ -ASEP. To indicate the position of RNAP on DNA track, we use the leftmost site among the ℓ successive sites covered by the RNAP. Let $Q(\underline{i}|j)$ be the conditional probability that, given a RNAP at site i

(expressed by the underbar), there is no RNAP at site j . Suppose $P_\mu(i, t)$ is the probability of finding the RNAP in μ_{th} chemical state at i_{th} nucleotide at time t , then time evolution of these probabilities $P_\mu(i, t)$ are governed by master equations [26] that incorporate the effective steric interaction felt by each RNAP.

Under periodic boundary condition (PBC), the number density ρ of the RNAPs is conserved. Solving the master equations under the steady state condition one can calculate the flux of the RNAPs analytically. Since in each polymerization step, mRNA is elongated by one nucleotide, RNAP flux also represents the net rate of mRNA synthesis. In figure 3, flux J is plotted against the coverage density ($\rho_{cov} = \rho\ell$) of RNAP, for a few different values of NTP concentration. Because of the extended size of the RNAP particles, the flux-density relation is asymmetric about $\rho = 1/2$.

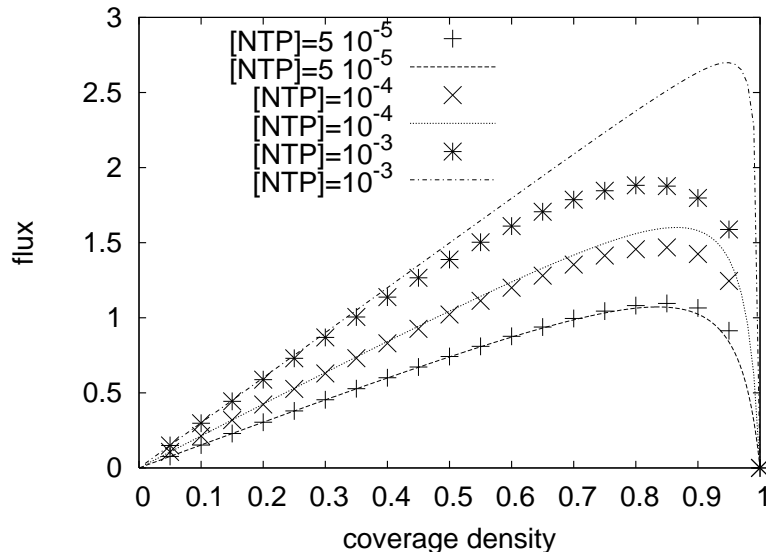


FIG. 3: RNAP flux is plotted for a few values of NTP concentration. Solid lines corresponds to the theoretical prediction whereas discrete data are obtained from the simulation. The values of other parameters are $\omega_{21}^f = 10^6 [NTP] s^{-1}$, $\omega_{11}^f = 46.6 [NMP] s^{-1}$, $\omega_{22}^f = .31 [NTP] s^{-1}$, $\omega_{21} = 10^6 [PP_i] s^{-1}$, $\omega_{12} = 31.4 s^{-1}$, $\omega_{12}^b = .21 s^{-1}$, $\omega_{11}^b = .94 s^{-1}$, $\omega_{22}^b = .063 s^{-1}$ and $[PP_i] = 1 \mu M$ (adapted from ref.[26]).

Very recently the effects of RNAP traffic congestion on the backtracking of individual RNAPs and kinetic proofreading have also been studied theoretically [42]. In the Sahoo-Klumpp model of nucleolytic proofreading during transcription [42], a rigid rod that represents a RNAP and has step size unity in the units of a single base. Upon incorporation of an incorrect nucleotide, it makes a transition to the “error state” with rate p without forward translocation (see fig.4). Alternatively, even after such a misincorporation, it can translocate forward with a rate that is lower than its normal rate of forward translocation (which is accompanied by the incorporation of a correct nucleotide). Once in the “error state”, the RNAP can backtrack; in this state it moves in a diffusive manner. Elongation can resume along two alternative routes. The RNAP can either regain its active position and then resume elongation (thereby leaving the erroneously incorporated nucleotide intact) or cleave the transcript at its backtracked position and occupy the newly created active state (thereby resuming elongation after correcting the error) (see fig.4). Sahoo and Klumpp [42] calculated the fraction of the errors that are corrected by backtracking and transcript cleavage. This process, when carried out by a single RNAP without hindrance or obstruction from any other RNAP, is similar to that studied earlier by Voliotis et al.[41] by a slightly different set of mathematical steps. However, Sahoo and Klumpp studied the more general scenario by taking into account the effects of steric interactions of the RNAPs in a congested RNAP traffic. In such a situation success of error correction hinges on the rate of cleavage; this rate has to be sufficiently high so that erroneously incorporated nucleotide is cleaved before the backtracked RNAP get reactivated by a trailing RNAP.

IV. DDDP AND DNA REPLICATION

Most of the DNA polymerases have a “cupped right hand”-like structure where its sub domains can be identified as palm, thumb and finger domain. Shapes and sizes of these sub domains vary extensively from polymerase to

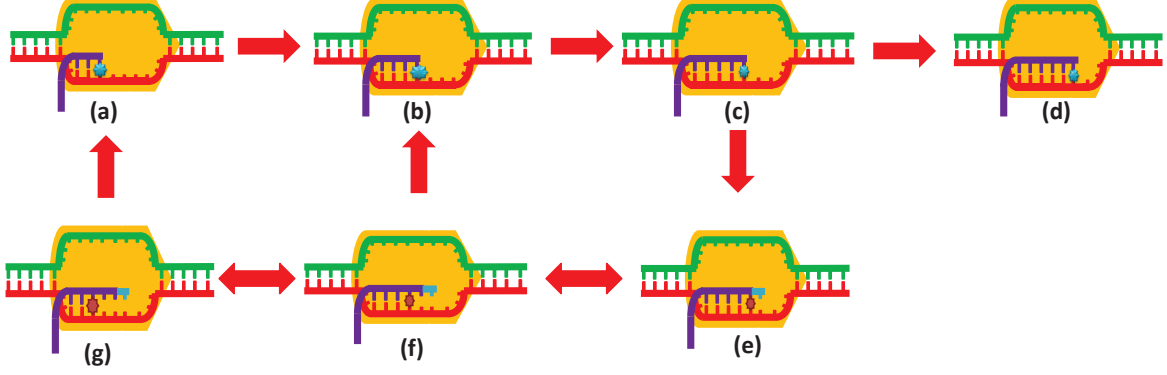


FIG. 4: Cartoon diagram of backtracking and kinetic proofreading during transcription. Active RNAP (state a) incorporates two successive correct nucleotides and reaches into state (c). After an incorrect incorporation it jumps in the error state (e), without any translocation. From error state (e), RNAP may backtrack to the previous site. In backtracked state RNAP has the equal probability for forward and backward motion. This backtracked state may also cleave the erroneous part of the nascent polynucleotide which result in the transition to the active state of RNAP.

polymerase but overall structure remains the same. The template strand enters through the finger domain and exits from the thumb domain, while the dNTP binds between finger and palm domain.

A. Single DDDP: speed and fidelity of DNA replication

In their pioneering *in-vitro* experiments on DDDP, Wuite et al. [50] applied tension on a ssDNA molecule, that served as the template, by holding it with a micro pipette at one end and an optical trap on the other. Similar experiments were carried out, almost simultaneously, by Maier et al.[51] on a different DNAP and using a magnetic trap. In these experiments, the ssDNA was converted into a dsDNA by the DDDP. Interestingly, the average rate of replication $k(F)$ was found to vary nonmonotonically with the tension F [50, 51]. The observed trend of variation of the replication rate was explained in terms of the differences in the force-extension curves of ssDNA and dsDNA [50, 51]. An alternative model developed by Goel et al.[52, 53] has been further elaborated by an atomistic model, that was studied computationally, by Andricioaei et al. [54].

A DDDP is a dual-purpose enzyme that plays two opposite roles in two different circumstances during DNA replication. It plays its normal role as a polymerase catalyzing the *elongation* of a new DNA molecule. However, it can switch its role to that of an exonuclease catalyzing the *shortening* of the nascent DNA by cleavage of the nucleotide at the growing tip of the elongating DNA [55]. The two distinct sites on the DNAP where, respectively, polymerization and cleavage are catalyzed, are separated by 3-4 nm [56]. The nascent DNA is transferred back to the site of polymerization after cleaving the nucleotide from its growing tip. The elongation and cleavage reactions are thus *coupled* by the transfer of the DNA between the sites of polymerase and exonuclease activity of the DNAP. However, the physical mechanism of this transfer is not well understood [39]. “Exo-deficient” mutants and “transfer-deficient” mutants have been used to understand the interplay of exonuclease and transfer processes on the platform of a single DDDP [56].

Normally, transfer of the nascent DNA from the polymerase site to the exonuclease site takes place upon incorporation of a wrong nucleotide so that the misincorporated nucleotide can be cleaved off. However, in spite of this quality control system, some misincorporated nucleotides can escape cleavage; such *replication error* in the final product is usually about 1 in 10^9 nucleotides. Moreover, one cannot rule out the possibility of a similar transfer, albeit rarely, even after the incorporation of a correct nucleotide. If in this process the correct nucleotide is erroneously cleaved off before getting transferred back to the polymerase site, such “futile” cycles of the DDDP would unnecessarily slow down the replication process [57].

Fig.5 depicts, a minimal three-state kinetic model [58] of DNA polymerase on leading strand, where the continuous replication take place. In this model correct and incorrect nucleotides follow the same kinetic path but the rate constants for chemical transition differs significantly, making the correct incorporation more favorable. Rate constants for correct and incorrect nucleotides are represented by ω and Ω , respectively, and the same subscripts are used for the same type of transitions. In the figure 5, chemical state 1 represents the state where DNA polymerase is ready for the next round of elongation cycle. The transition $1 \rightarrow 2$ stands for polymerization step, occurs with rate $\omega_f(\Omega_f)$

for correct(incorrect) nucleotides.

In principle, the transition $1 \rightarrow 2$ can be divided into more than one sub steps[59]. These sub steps are shown in figure 6. In figure 6, E_c and E_o denote the closed and open conformation of the DNA polymerase, whereas D_n represent the position of the catalytic site. When a substrate (dNTP) binds with DNAP, its binding energy transforms the DNAP from an open configuration to a close configuration. This new configuration of the DNAP favors the formation of diester bond. As a result of the polymerization reaction the nascent DNA is elongated by one nucleotide. This sub-step is followed by switching of the DNAP to the open conformation and the release of PP_i , thereby completing the $1 \rightarrow 2$ transition. Random fluctuations between open and closed conformations of DNAP may drive the reaction in backward direction causing the disassociation of dNTP by rate $\omega_r(\Omega_r)$ for correct (incorrect) nucleotide.

The transition $2(E_o + D_{n+1}) \rightarrow 1(E_o D_{n+1})$ symbolizes the relaxation of the last incorporated nucleotide with rate $\omega_h(\Omega_h)$ for correct (incorrect) nucleotide incorporated. Chemical state $2(E_o + D_{n+1})$ may activate the exonuclease mode of the enzyme (state 3) by transferring the growing DNA chain to exonuclease site at the rate $\omega_{pf}(\Omega_{pf})$ for correct(incorrect) nucleotide. The active exonuclease site can cleave the last incorporated nucleotide with rate $\omega_e(\Omega_e)$ for correct (incorrect) incorporation, alternatively it may also switch back to polymerase active mode with rate $\omega_{pr}(\Omega_{pr})$ for correct (incorrect) incorporation. For this model, Sharma and Chowdhury [58] derived the distribution of the dwell times and that of the exonuclease turnover times. The exact analytical expressions for these distributions display the effect of the coupling of two different enzymatic activities of a DNAP, namely, its polymerase activity and exonuclease activity.

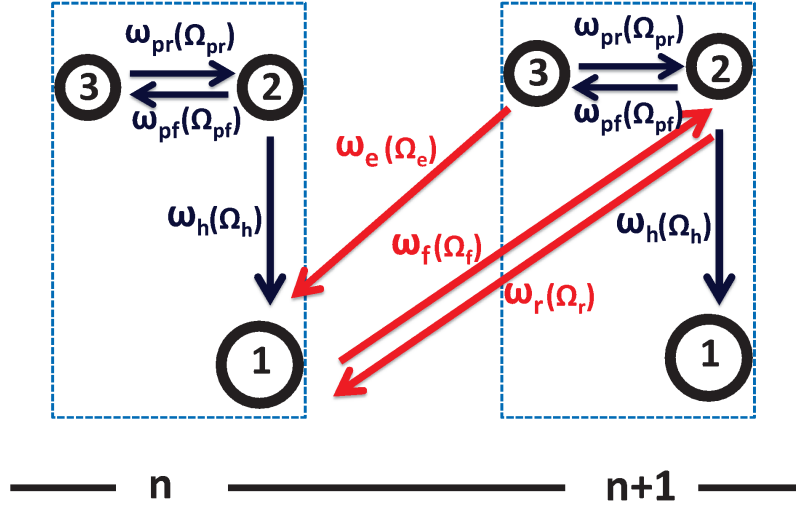


FIG. 5: Full mechano-chemical cycle in the model of DNAP developed by Sharma and Chowdhury [58] (see the text for details).



FIG. 6: Sub-steps in the transition $1 \rightarrow 2$ shown in fig.5 (see the text for details).

Unlike RNAP, the DNAP is not capable of helicase activity. Therefore, ahead of the DNAP, a helicase progressively unzips the dsDNA thereby exposing the two single strands of DNA which serve as the templates for DNA replication (see fig.7). For the processive translocation of a DNAP on its template, it needs to be clamped with a ring-like “DNA clamp” [60]. The assembly of a DNA clamp is assisted, in turn, by a “clamp loader” in a ATP-dependent manner [61–65]. DNAP cannot initiate replication on its own and requires priming by another enzyme called primase (see fig.7) [66]. Thus, DDDPs alone cannot replicate the genome; together with DNA clamp and clamp loader, DNA helicase and primase, it forms a large multi-component complex machinery which is often referred to as the *replisome* [67–80]. The spatio-temporal coordination of the operation of the different components of the replisome during DNA replication is the most interesting aspect of its operational mechanism.

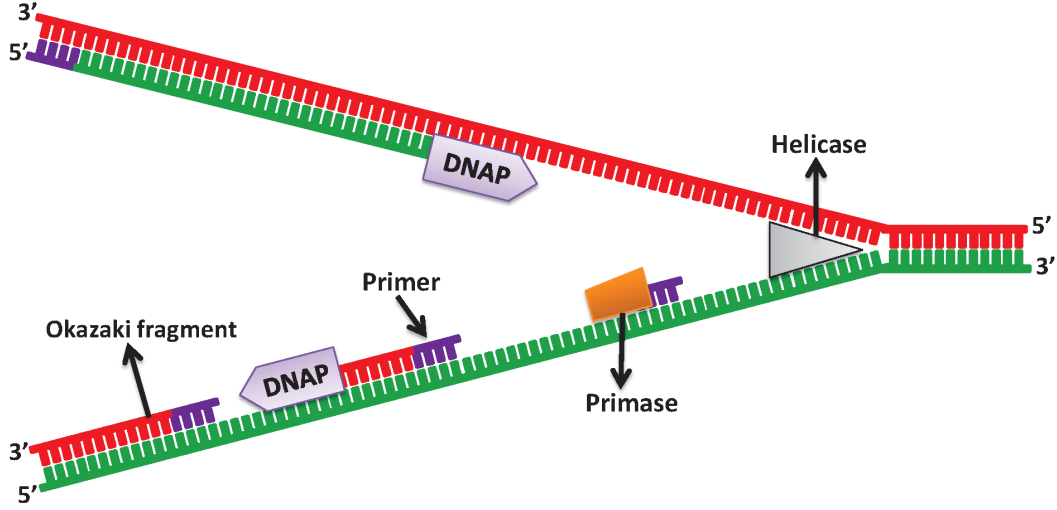


FIG. 7: DNA replication process (see text for details).

B. Coordination of two replisomes at a single fork

DNA replication is more complex than transcription. Two DDDPs have to replicate these two complementary strands of DNA. However, each DDDP is capable of translocating only unidirectionally ($5' \rightarrow 3'$) for elongating the corresponding product strand. As a result, one of the strands (called the “leading strand”) is synthesized processively, whereas the “lagging strand” is replicated discontinuously; processing of these “Okazaki fragments” into a continuous DNA strand takes place in three steps catalyzed by three enzymes which are not part of the replisome (see fig.7).

How are the replication of the leading and lagging strands maintain tight coordination as the replication fork moves forward? Does the DNAP on the lagging strand polymerize at a faster rate than that on the leading strand so as to make up for the time lost in the priming and in re-starting DNA elongation thereby enabling it to catch up the DNAP on the leading strand? Or, does the DNAP on the leading strand make a pause at the replication fork during the interval between the end of synthesis of one Okazaki segment and the beginning of that of the next Okazaki segment on the lagging strand? Experimental investigations, particularly, single-molecule experiments, have started addressing these questions in the recent years. For example, it has been found that the primase acts, at least effectively, as a molecular “brake” preventing the leading-strand synthesis from outpacing the lagging-strand synthesis of DNA [81, 82].

V. RDRP OF RNA VIRUSES AND RNA REPLICATION

RNA viruses contain a small genome that is usually not longer than 30kb. It may consist of either a ssRNA or a dsRNA. In some viruses RNA genome consists of more than one segment whereas in others it is a single segment. In multi segment RNA viruses, all the genome segments are replicated independently.

In spite of strong resemblance of the overall shape of all the RDRPs with a “cupped right hand”, viral RDRPs have some special architectural features [83–86]. The most notable distinct feature of these polymerases is that, in contrast to the “open hand” shape of the other polynucleotide polymerases, the RDRP resembles a “closed hand”. The closing of the “hand” is achieved by loops, called “fingertips”, which protrude from the fingers and connect with the thumb domain at their other end. The fingertip region forms the entrance of the channel where the RDRP binds with the RNA template. In addition, there is a small positively charged tunnel through which the nucleotide monomers, required for elongation of the RNA, enter.

RDRP reads the template by moving along the 3 to 5 direction on the template RNA while simultaneously synthesizing the complementary RNA from 5 to 3 direction[87]. The genome of some of the viruses consist of double stranded RNA; the corresponding RDRP have some additional unique structural elements which unzip the two strands and feed the appropriate strand to the catalytic site.

RDRPs in different systems are known to adopt distinct strategies of initiation [88]; these include both (i) *Primer*

independent initiation as well as (ii) *Primer dependent initiation*. In the latter case several different potential sources of primers have been identified. For example, (a) an oligonucleotide discarded as a result of abortive initiation can serve as a primer; (b) an oligonucleotide generated by the cleavage of the 5' end of a mRNA of the host cell can also be exploited as a primer; (c) the 3' end of the looped template itself can be utilized as the primer.

VI. RDDP OF RETROVIRUSES AND REVERSE TRANSCRIPTION

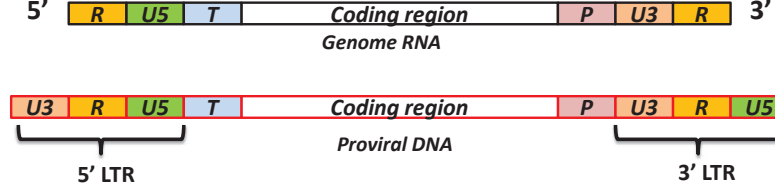


FIG. 8: Sequence of the genomic RNA and proviral DNA are shown schematically (adapted from [89]). Different regions of these sequences are represented by different colors. R is the directly repeated sequence found at both termini of the genome RNA but is internal to the proviral DNA. U3 and U5 are unique sequences located near the 3' and 5' ends of the genomic RNA, respectively. Combination of U3, R and U5 is known as long terminal repeats (LTR). T is complementary to the host tRNA (primer for reverse transcription) and P is polypurine rich region, which is relatively resistant to the RNaseH activity of RT.

Recall that transcription is the process whereby a RNA strand is polymerized using a DNA strand as the template. Therefore, the reverse process, i.e., polymerization of a DNA strand using RNA template was given the name “reverse transcription” and the corresponding polymerase is called a reverse transcriptase (RT).

Reverse transcription is a crucial step in the life cycle of retroviruses [90]. Research on retroviruses got an enormous boost in the mid-1980s after AIDS became one of the main focus of research in virology and medicine. Obviously, most of the research on RT over the last four decades has been dominated by studies of the RT of human immunodeficiency virus (HIV) [91]. RT of HIV is one of key targets for the some of the drugs which are being tried against AIDS. Nevertheless, impressive progress have been made also in understanding the structure and function of non-HIV RTs [92].

Strictly speaking, a RT performs three distinct tasks [93] (see fig.9): (i) reverse transcription: RT polymerizes a DNA strand using the genomic RNA as the corresponding template (i.e., the process from which it derives its name); (ii) RNaseH activity: RT cleaves the RNA strand of the DNA-RNA duplex formed by the process (i) above; (iii) DNA polymerase: RT also plays the role of a DDDP by catalyzing the polymerization of a DNA strand that is complementary to the DNA strand synthesized in the process (i) above.

Thus, a RNA strand, which constitutes the viral genome, serves only as the initial template and the final product of reverse transcription is called a proviral DNA (see fig.8).

Structural studies of RT have revealed that DNA polymerase domains of the RT are similar to the DNA polymerases of living cells. But, the RT also has some additional distinct features which are responsible for its RNaseH activity. The Catalytic domains that perform the Polymerase and RNaseHase activities of a RT are spatially distinct, but are linked through the “connection subdomain” [93]. RT of HIV binds with substrate in two different orientations each of which is capable of DNA polymerase and RNaseH activities. Switching of the orientations switch the RT activity [95]. This switching occurs spontaneously and it is regulated by the small ligand molecules.

Majority of the RTs use host tRNA as the required primer. But, some RTs use other resources for priming [96]. RT is deficient in proofreading capabilities [97]. Consequently, the rate of reverse-transcriptional error is quite high. Since completion of the integration of the provirus into the host genome involves several steps driven by the RT, the errors of each step add up. Higher mutation rate in retroviruses has severe consequences- the virus uses it as one of its survival strategies against the host defence system whereas the host immune systems finds it difficult to recognize it. A kinetic model for the stochastic description of the process of reverse transcription by RT has been formulated [98]

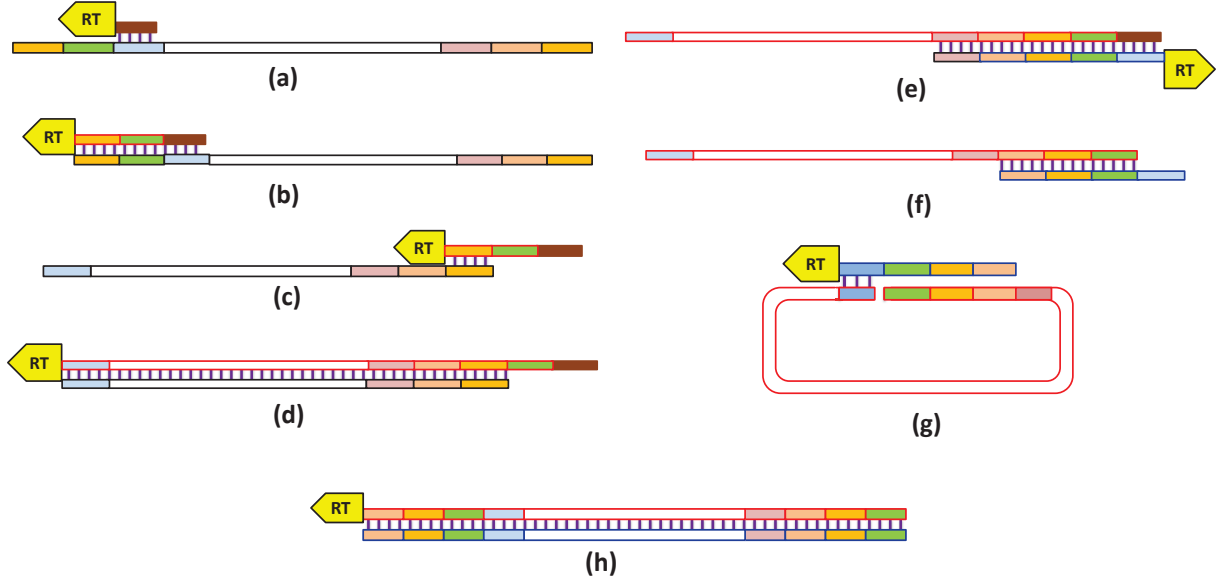


FIG. 9: Schematic diagram of reverse transcription (adapted from [94]) Different polynucleotids are represented by the boundaries of different colors. RNA genome have black boundary whereas positive sense and negative sense DNA strands are covered by red and blue boundaries, respectively. (a) tRNA molecule forms the base pairs with T and works as a primer to initiate the reverse transcription. (b) Primer is extended by RT till the 5' end of the genome. (c) While elongating the DNA, RNase H activity of RT digests the template RNA by leaving the DNA free from base pairing. So the DNA re-associate with the sequence R at the 3' end of the RNA genome, known as first template switch. (d) RT elongates the DNA till 5' end of the genome. (e) RNA exist in the DNA-RNA duplex is degraded by the RNase H activity of the RT except the sequence P which works as a primer for the initiation of the positive strand synthesis. RT elongates the DNA till the end of template at tRNA. (f) Now the tRNA and region P are degraded by RNase H activity of RT. (g) The DNA strand form a loop which gives the opportunity to form a base pair between the T region of both strands. (h) After the positive strand transfer both DNA strands are elongated till the ends of their template.

VII. INTERFERENCE OF TRANSCRIPTION AND REPLICATION: TRAFFIC RULES FOR RNAP-DNAP COLLISION

Transcription of a gene is carried out a large of times during the life time of a single cell. In contrast, a distinct feature of DNA replication is that, during its lifetime, a cell must not replicate its genome more than once. Only recent investigations have explored how cell achieves this requirement. Replication of bacterial genome (e.g., E-coli) proceeds *bidirectionally* from the initiation site (oriC). Each replication fork, alongwith its replisome synthesizing the leading and lagging strands approaches the same termination site (terC), but from opposite directions. As the replication forks move, there is a possibility for collision with a TEC on the way if a gene is getting transcribed simultaneously (see Fig.10).

When a replication fork follows a leading TEC, the DNAP remains stalled as long as the leading RNAP pauses on its track; however, the DNAP resumes replication once the RNAP starts moving forward again [99]. Similarly, if the replication fork collides with the TEC *head-on* from opposite direction, the DNAP can bypass the moving RNAP [100].

VIII. RIBOSOMES AND POLYMERIZATION OF POLYPEPTIDES

Ribosome, one of the largest and most sophisticated macromolecular machines within the cell, polymerizes polypeptides using a mRNA as the corresponding template [102–106]. In each successfully completed mechano-chemical cycle of a ribosome two molecules of guanosine triphosphate (GTP) are hydrolyzed into guanosine diphosphate (GDP). Moreover, one of the steps of this cycle needs the assistance of specifically prepared molecular assembly whose preparation also involves hydrolysis of a molecule of ATP. Because of these energy-consuming steps involved in the operation of a ribosome, it is regarded as a molecular motor [107].

A “slippage” of the reading frame by $3n$ nucleotides, where n is an integer, would result in missing n amino acids without affecting the identity of the other amino acids. However, if the slippage is not a multiple of 3 nucleotides, the

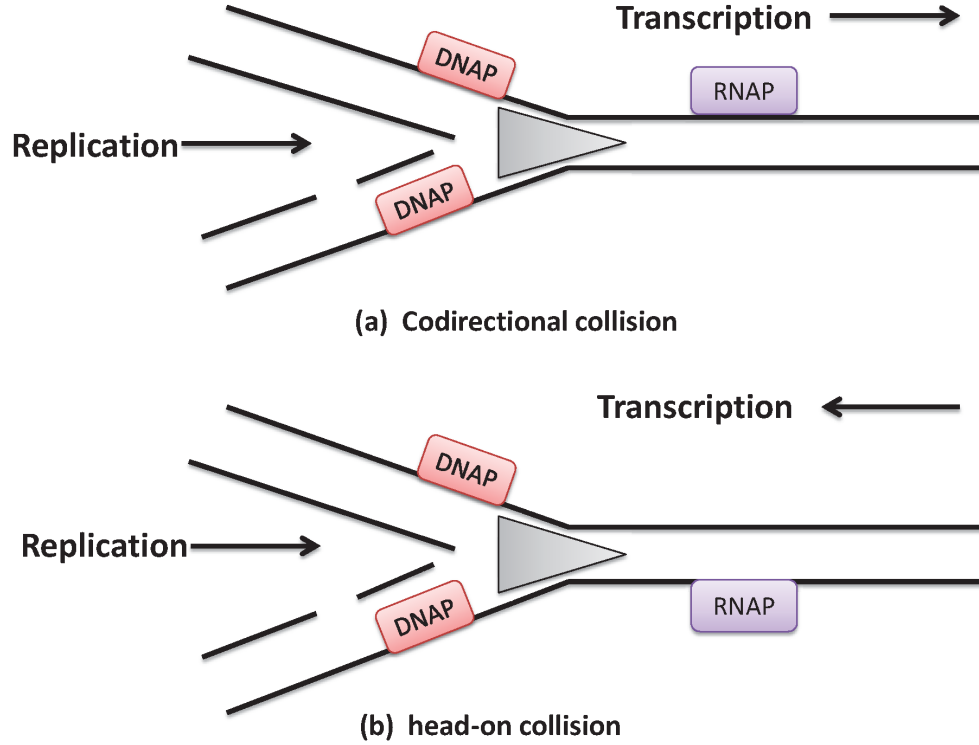


FIG. 10: Schematic representation of collision between replication fork and TEC (a) codirectional collision: replication fork and TEC move in the same direction and RNAP transcribes the leading strand. (b) head-on collision: replication fork and TEC move in opposite direction and RNAP transcribes the lagging strand (inspired by ref.[101]).

entire sequence of amino acids after the slippage would be different from the coded sequence.

Aminoacyl tRNA synthetase (aa-tRNA synth) “charges” a tRNA molecule with a amino acid. In order to ensure high fidelity of translation, the aa-tRNA synth must have high specificity for its two substrates, namely, tRNA and amino acid [108]. The error committed by aa-tRNA synth never exceeds once in 10^4 enzymatic cycles. Interestingly, aminoacyl-tRNA synthetase and DNAP share some common mechanisms to ensure translational and replicational fidelities, respectively [109].

It has been argued [102] that the energy of the chemical bond between the amino acid and tRNA is later used by the ribosome for forming a peptide bond between this amino acid and the nascent polypeptide. The free energy released by the hydrolysis of two GTP molecules are utilized, respectively, in selecting the correct aa-tRNA and the release of the deacylated tRNA into the surrounding aqueous medium.

A. Composition and structure of a single ribosome

Even in the simplest organisms like single-cell bacteria, a ribosome is composed of few rRNA molecules as well as several varieties of protein molecules. The structure of both bacterial and eukaryotic ribosomes have been revealed by extensive detailed investigation over several years by a combination of X-ray diffraction, cryo-electron microscopy, etc. [110–123]. For this achievement, V. Ramakrishnan, T.A. Steitz and A. Yonath shared the Nobel prize in chemistry in 2009 [113, 115, 118]. For many years the mechano-chemical kinetics of ribosomes have been investigated by studying bulk samples with biochemical analysis as well as the structural probes mentioned above. Only in the last few years, it has been possible to observe translation by single isolated ribosome *in-vitro* [124–135].

Ribosomes found in nature can be broadly divided into two classes: (i) prokaryotic 70S ribosomes, and (ii) eukaryotic 80S ribosomes; the numbers 70 and 80 refer to their sedimentation rates in the Svedberg (S) units. In the earliest electron microscopy the prokaryotic and eukaryotic ribosomes appeared to be approximately spherical particles of typical diameters in the ranges 20 – 25 nm and 20 – 30 nm, respectively. In these electron micrographs a visible groove was found to divide each ribosome into two unequal parts; the larger and the smaller parts are called, for

obvious reasons, large and small subunit, respectively. The sizes of the large and small subunits of the 70S ribosome are 50S and 30S respectively, whereas those of the 80S ribosome are 60S and 40S, respectively.

The small subunit binds with the mRNA track and assists in decoding the genetic message encoded by the codons (triplets of nucleotides) on the mRNA. The “head” and the “body” are the two major parts of the *small* subunit. Two major lobes, which sprout upward from the “body”, are called the “platform” and the “shoulder”, respectively. The decoding center of the ribosome lies in the cleft between the “platform” and the “head” of the small subunit. The incoming template mRNA utilizes a “channel” formed between the “head” and the “shoulder” as a conduit for its entry into the ribosome. Through the cleft between the “head” and the “platform” the mRNA exits the ribosome.

But, the actual polymerization of the polypeptide takes place in the large subunit. The characteristic “crown-like” architecture of the *large* subunit arises from three protuberances. On the flat side of the large subunit exists a “canyon” that runs across the width of the subunit and is bordered by a “ridge”. Halfway across this ridge, a hole leads into a “tunnel” from the bottom of the “canyon”. This “tunnel” penetrates the large subunit and opens into the solvent on the other side of the large subunit. This “tunnel” serves as the conduit for the exit of the nascent polypeptide chain. This “tunnel” is approximately 10 nm long and its average width is about 1.5 nm.

Several intersubunit “bridges” connect the two subunits of each ribosome. These bridges are sufficiently flexible so that relative movements of the two subunits can take place in each cycle of the ribosome. The intersubunit space is large enough to accommodate just three tRNA molecules which can bind, at a time, with the three binding sites designated as E, P and A. Moreover, the shape of the intersubunit space is such that it allows easy passage of the L-shaped tRNA molecules. The operations of the two subunits are coordinated by the tRNA molecules.

B. Mechano-chemical kinetics of a single ribosome: speed and fidelity of translation

A ribosome may translate at the rate of a few codons to few tens of codons per second. Just like the synthesis of polynucleotides (e.g., transcription and replication), synthesis of polypeptides (i.e., translation) also goes through three stages, namely, *initiation*, *elongation*, and *termination*.

During the elongation stage, while translating a codon on the mRNA template, the three major steps in the mechano-chemical cycle of a ribosome are as follows (see fig.11): In the first, based on matching the codon with the anticodon on the incoming aa-tRNA, the ribosome *selects* the correct amino acid monomer that, according to the genetic code, corresponds to this codon. Next, it catalyzes the chemical reaction responsible for the formation of the peptide bond between the nascent polypeptide and the newly recruited amino acid resulting in the *elongation* of the polypeptide. Final step of the cycle is *translocation* at the end of which the ribosome finds itself at the next codon and is ready to begin the next cycle.

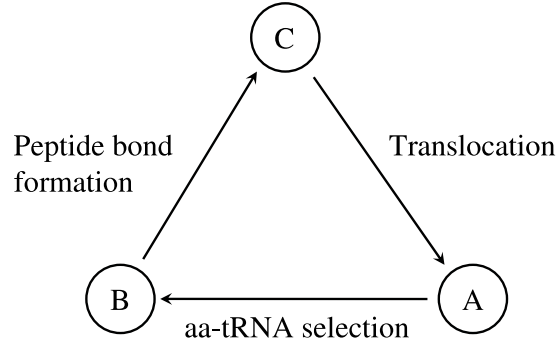


FIG. 11: Pictorial depiction of the three main stages in the chemo-mechanical cycle of a single ribosome (see the text for details).

Thus, each ribosome has three distinct functions which it performs on each run along the mRNA track:

- (i) it is a *decoding device* in the sense that it “reads” the genetic message encoded in the sequence of codons on the template mRNA and selects the correct corresponding amino acid monomer;
- (ii) it is a *“polymerase”* because it elongates the polypeptide chain by one amino acid by catalyzing the formation of the peptide bond between the nascent polypeptide and the newly recruited amino acid;
- (iii) it is a *motor* that steps forward by one codon on a mRNA strand by transducing chemical energy into mechanical work.

Interestingly, function (i) is performed exclusively by the smaller subunit while the function (ii) is carried out in the larger subunit. But, the function (iii) requires coordinated movement of the two subunits by tRNA molecules.

Elongation factors (EF), which are themselves proteins, play important roles in the control of the three major steps shown in fig.11. During the process of checking its identity through the codon-anticodon matching (which takes place in the smaller subunit), the formation of the peptide bond is prevented by an elongation factor Tu (EF-Tu). However, once a cognate tRNA is identified, the smaller subunit sends a “green signal” (by a molecular mechanism that remains unclear), the EF-Tu separates out by a process driven by GTP hydrolysis thereby clearing the way for the peptide bond formation. Similarly, elongation factor G (EF-G) coordinates the translocation of the mRNA by one codon and the simultaneous movement of the tRNA molecules from one binding site to the next one. Thus, the hydrolysis of the first GTP molecule is exploited for the selection of the correct aminoacyl-tRNA at the A site whereas that of the second GTP molecule is utilized to release of the deacylated tRNA molecule from the E site.

Clearly, the 3-state cycle sketched in fig.11 is an oversimplified description of the mechano-chemical kinetics of a ribosome during the elongation stage. We’ll see in this section that at least two of the three steps in fig.11 consist of important sub-steps. Moreover, the aa-tRNA selected (erroneously) by the ribosome may not be the correct (cognate) tRNA. Rejection of such non-cognate and near-cognate tRNAs by the process of kinetic proofreading leads to an alternative branch completion of which ends up in a futile cycle. The roles played by some of the key devices sketched in fig.12, which we explain below, have to be captured by a more detailed model of translation. Next we review such a modeling strategy.

1. Selection of amino-acid: two sub-steps

Selection of an amino acid by a ribosome is a two-step process and these steps are (i) initial selection and (ii) kinetic proofreading. Elongation cycle of the ribosome starts with chemical state 1, shown in figure 13. In this state growing polypeptide chain is attached with the site P of the large subunit of ribosome whereas site E and A remain empty. An initial selection begins when a tRNA along with an amino acid subunit, elongation factor EF-Tu and a GTP molecule binds with the site A of the large subunit. This binding result in the transition to chemical state 2 with rate ω_a . All species of tRNAs, depending upon their relative concentration in the solution, compete with each other to bind with the ribosome, but in order to ensure the optimum fidelity, most of the non cognate and some near cognate tRNAs are rejected on the basis of codon-anticodon matching. This rejection result in the $2 \rightarrow 1$ transition, with rate ω_{r1} . If a tRNA is not rejected then this binding stabilizes the ribosome complex and transmit a signal to EF-Tu to hydrolyze the GTP molecule. Then the GTP molecule is hydrolyzed and corresponding irreversible transition $2 \rightarrow 3$, occurs with rate ω_{h1} . This hydrolysis process is followed by some structural rearrangements in ribosome, which result in the release of the non cognate and near cognate tRNAs along with the EF-Tu and GDP molecule. This irreversible step $3 \rightarrow 1$ occurs by rate ω_{r2} and often referred as kinetic proofreading.

2. Peptide bond formation: peptidyl transfer

Sometimes an incorrect amino acid can escape from the two-stage quality control mechanism of ribosome, resulting an error in the final product. If the ribosome selects the correct amino acid it follows the main ($3 \rightarrow 4 \leftrightarrow 5 \rightarrow 1$) pathway but if the selected amino acid is incorrect then the relatively slow, branched ($3 \rightarrow 4^* \leftrightarrow 5^* \rightarrow 1$) pathway is followed. In the next step amino acid is bonded with growing polypeptide chain, and the GDP molecule as well as the protein elongation factor EF-Tu are released. Next, a new protein elongation factor EF-G along with along with a GTP molecule binds with the ribosome. For the correct amino acid this transition ($3 \rightarrow 4$) take place with rate ω_p , whereas for an incorrect amino acid it ($3 \rightarrow 4^*$) occurs with rate ω_p . Note that the only difference between $4(5)$ and $4^*(5^*)$ is that last incorporated nucleotide is correct in $4(5)$ but incorrect in $4^*(5^*)$.

3. Translocation: two sub-steps?

The next transition $4 \leftrightarrow 5$ ($4^* \leftrightarrow 5^*$) is the back and forth spontaneous Brownian rotation of the two subunits of the ribosome from a classical configuration (E/E,P/P,A/A) to hybrid configuration (E/P,P/A,A). This transition is purely driven by random thermal fluctuations without any external power supply. Forward transition occurs with rate $\omega_{bf}(\Omega_{bf})$, while the backward transition occurs with rate $\omega_{br}(\Omega_{br})$ for correct (incorrect) pathways. Finally the hydrolysis of the GTP along with translocation step results in $5 \rightarrow 1$ ($5^* \rightarrow 1$) transition with rate $\omega_{h2}(\Omega_{h2})$ for correct(incorrect) amino acid. This GTP hydrolysis completes one elongation cycle.

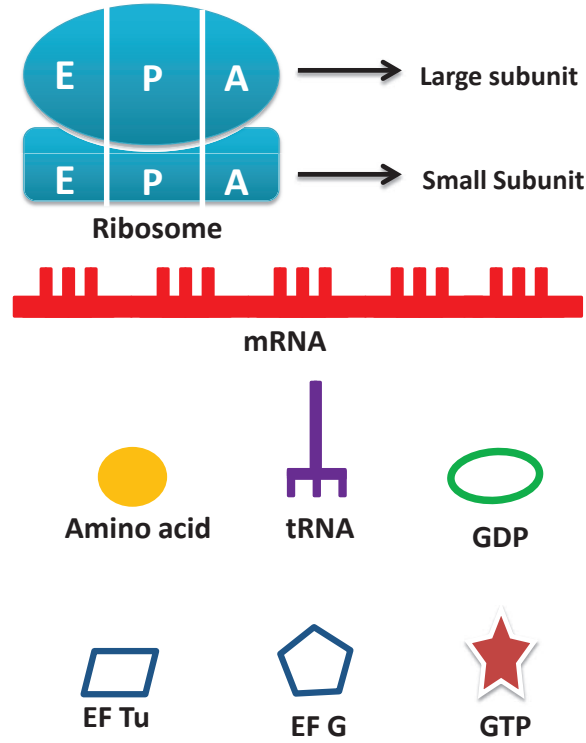


FIG. 12: Pictorial depiction of some of the key devices that participate in translation (see text for detailed explanation).

4. Dwell time distribution

As observed in single molecule experiments [124–135], the stochastic stepping of a ribosome is characterized by an alternating sequence of pause and translocation. The sum of the durations of a pause and the following translocation is defined as the time of a dwell of the ribosome at the corresponding codon. The codon-to-codon fluctuation in the dwell time of a ribosome arises from two different sources: (i) *intrinsic* fluctuations caused by the Brownian forces as well as the low of concentrations of the molecular species involved in the chemical reactions, and (ii) *extrinsic* fluctuations arising from the inhomogeneities of the sequence of nucleotides on the template mRNA [136]. Because of the sequence inhomogeneity of the mRNA templates used by Wen et al. [134], the dwell time distribution (DTD) measured in their single-molecule experiment reflects a combined effect of the intrinsic and extrinsic fluctuations on the dwell time.

The probability density $f_{dwell}(t)$ of the dwell times of a ribosome, measured in single-molecule experiments [134], does not fit a single exponential thereby indicating the existence of more than one rate-limiting steps in the mechano-chemical cycle of each ribosome. Best fit to the corresponding simulation data was achieved assuming five different rate-determining steps [135].

We'll now sketch a theoretical framework [137, 138] which provides an exact analytical expression for $f_{dwell}(t)$ in terms of the rate constants for the individual transitions in the mechano-chemical kinetics of a single ribosome. This scheme also involves essentially five steps in each cycle during the elongation stage of translation. However, for the sake of simplicity of analytical derivation of the exact expression for $f_{dwell}(t)$, this theory assumed the template mRNA to have a *homogeneous* sequence (i.e., all the codons of which are identical).

If we start our clock ($t = 0$) when a ribosome is in chemical state 1 at site i , then the time taken by the ribosome to reach the chemical state 1 of $(i + 1)th$ site is defined as the dwell time of the ribosome. Let us assume that $P_\mu(i, t)$ is the probability of finding the ribosome in μ_{th} chemical state at site i , at time t . For a single ribosome time evolution of the probability $P_\mu(i, t)$ are governed by the corresponding master equations [138].

For the calculation of the dwell time following initial conditions are imposed:

$$P_1(i, 0) = 1 \text{ and } P_2(i, 0) = P_3(i, 0) = P_4(i, 0) = P_5(i, 0) = P_4^*(i, 0) = P_5^*(i, 0) = P_1(i + 1) = 0 \quad (1)$$

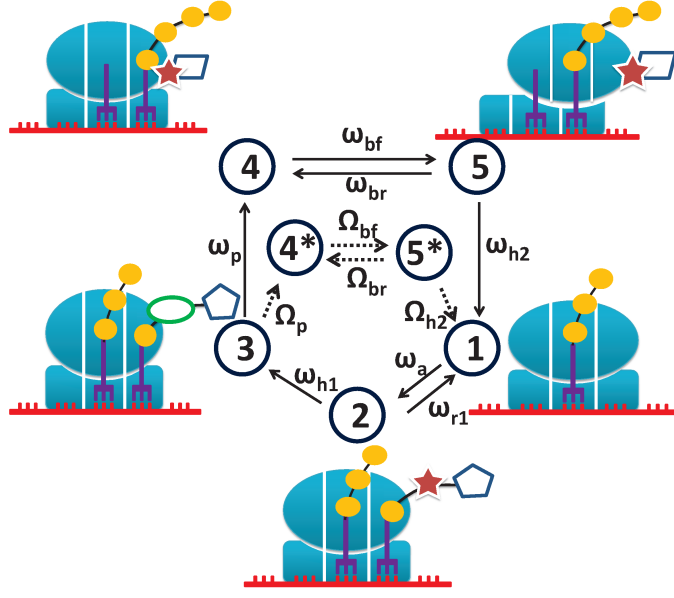


FIG. 13: Pictorial depiction of the full mechano-chemical cycle of the ribosome

The probability density of the dwell times $f_{dwell}(t)\Delta t$ can be obtained from

$$f_{dwell}(t) = \frac{dP_1(i+1, t)}{dt} = \Omega_{h2}P_5^*(i, t) + \omega_{h2}P_5(i, t) \quad (2)$$

In the translation process many ribosomes move on the same *mRNA* track and each of them synthesizes a separate copy of the same protein. Their steric interaction can be captured by appropriately modifying the master equations.

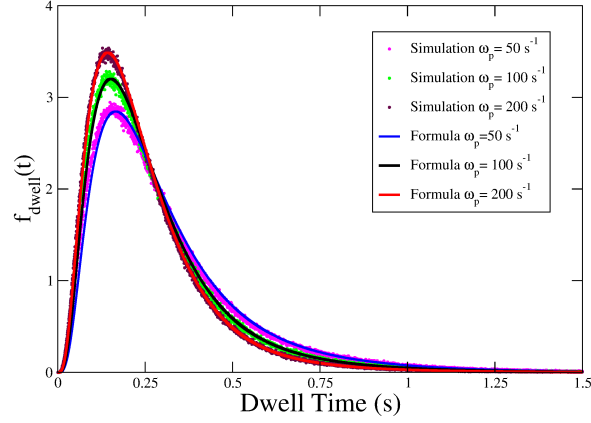


FIG. 14: Dwell time distribution of ribosome is plotted for a few different values of ω_p . The values of other rate constants are $\omega_a = 25\text{s}^{-1}$, $\omega_{r1} = 10\text{s}^{-1}$, $\omega_{h1} = 25\text{s}^{-1}$, $\omega_{r2} = 10\text{s}^{-1}$, $\Omega_p = 40\text{s}^{-1}$, $\omega_{bf} = \omega_{br} = 25\text{s}^{-1}$, $\Omega_{bf} = \Omega_{br} = 10\text{s}^{-1}$, $\omega_{h2} = 25\text{s}^{-1}$, $\Omega_{h2} = 10\text{s}^{-1}$. The solid lines corresponds to the theoretical prediction whereas the discrete points corresponds to the data obtained by Monte Carlo simulation.

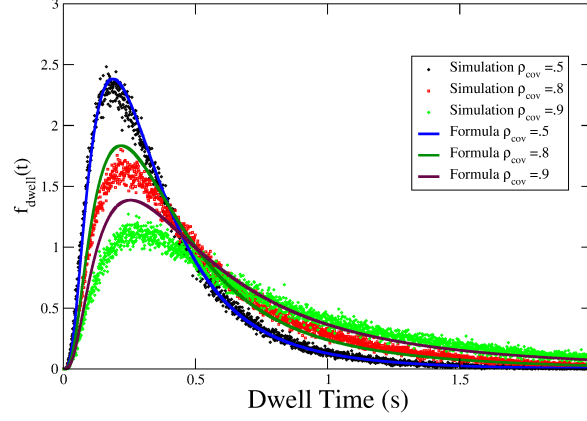


FIG. 15: Dwell time distribution of ribosome is plotted for a few different values of ρ_{cov} . The values of other rate constants are $\omega_a = 25\text{s}^{-1}$, $\omega_{r1} = 10\text{s}^{-1}$, $\omega_{h1} = 25\text{s}^{-1}$, $\omega_{r2} = 20\text{s}^{-1}$, $\omega_p = 50\text{s}^{-1}$, $\Omega_p = 40\text{s}^{-1}$, $\omega_{bf} = \omega_{br} = 25\text{s}^{-1}$, $\Omega_{bf} = \Omega_{br} = 10\text{s}^{-1}$, $\omega_{h2} = 25\text{s}^{-1}$, $\Omega_{h2} = 10\text{s}^{-1}$. The solid lines corresponds to the theoretical prediction whereas the discrete points corresponds to the data obtained by Monte Carlo simulation .

In figure 14 dwell time distribution of a ribosome is plotted for a few different values of ω_p . The same (or closely related) set of values of the parameters were used earlier also for the purpose of plotting. The selection of these values were motivated by typical magnitudes reported in the literature for various steps of translation (most often in bulk measurements). Higher value of ω_p decreases the value of the most probable dwell time. In figure 15 dwell time distribution of the ribosome is plotted for a few different values of ρ_{cov} . Due to the hindrance created by ribosome's mutual exclusion, higher value of ρ_{cov} leads to a longer most probable dwell time. The deviation of the theoretical prediction from the Monte Carlo data at higher coverage density is a consequence of the mean field approximation which ignores the correlations.

The expression for $f_{dwell}(t)$ thus derived incorporates the effects of fluctuations that are strictly *intrinsic*. This model [138] envisages a scenario that is very similar to the protocol used in some single-ribosome experiments [130] and is shown schematically in fig.16.

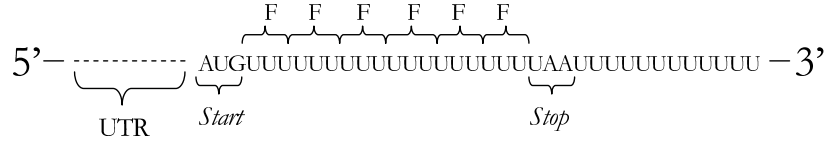


FIG. 16: A schematic description of a mRNA with homogeneous (poly-U) coding sequence (adapted from refs.[130, 131]).

The coding sequence to be translated consists of n_c number of identical codons. In the example shown of fig.16 $n_c = 6$ and each codon is UUU that codes for the amino acid Phenylalanine (which is denoted either by its abbreviation *Phe* or the symbol **F**). The coding sequence is preceded and followed by a start codon AUG and a stop codon UAA, respectively. A 5'-UTR precedes the start codon; this UTR is required for assembling the ribosome and for stabilizing the pre-initiation complex. At the 3'-end, after the stop codon there is a 3'-UTR consisting of a sequence of n_{nc} non-coding codons UUU ($n_{nc} = 4$ in the example of fig.16); this region merely ensures that the translation does not suffer from any "edge effect" when the ribosome approaches the 3'-end of the coding sequence. For such a poly-U mRNA sequence, aa-tRNA^{*Phe*} is the cognate aa-tRNA. Translational error can be studied using this protocol if, in addition to cognate aa-tRNA^{*Phe*}, near-cognate aa-tRNA^{*Leu*} is also supplied because the latter is cognate for the codon CUU which codes for *Leucine* (abbreviated **L**). An optical method, based on the labelling of the cognate, near-cognate and non-cognate tRNA molecules with dyes of different colors, has been suggested [138] to test the validity of the expression derived for $f_{dwell}(t)$.

C. Polysome: traffic-like collective phenomena

The collective movement of many ribosomes on a single mRNA strand is shown schematically in fig.17. It has superficial similarity with *single-lane uni-directional* vehicular traffic [139, 140] and is, therefore, sometimes referred to as ribosome traffic [141]. The ribosomes bound simultaneously to a single mRNA transcript are the members of a polyribosome (or, simply, *polysome*) [142–145]. Computer simulations of ribosome traffic have been carried out on a mRNA with a specially selected codon sequence near the start codon and allowing mRNA to decay at an optimum rate [146]. In this case, the metabolic cost of mRNA breakdown is more than compensated by the simultaneous increase in translation efficiency because of reduced queuing of the ribosomes.

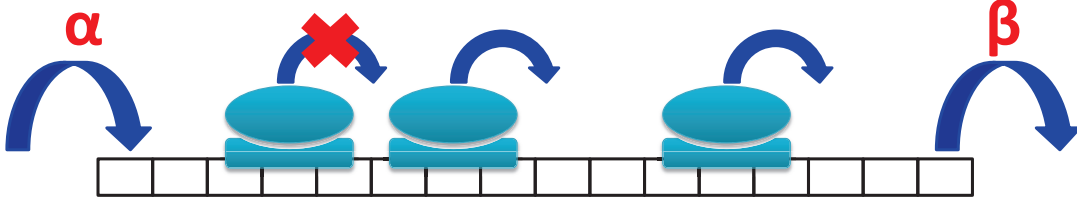


FIG. 17: Ribosome traffic on mRNA track is shown schematically. The parameters α and β denote the rates of translation initiation and termination, respectively. A ribosome can move forward by one codon if, and only if, the site immediately in front of it is not covered by another ribosome. The translation process is modelled more realistically by open boundary conditions, as shown here, than by periodic boundary conditions.

The polysome profiling technique [147, 148] provides the number of ribosomes bound to a mRNA, but not their individual positions where they remained “frozen” when translation was stopped by the experimental protocol. More detailed information on the numbers of ribosomes associated with specified *segments* of a particular mRNA can be obtained by using *ribosome density mapping* technique [149] which is based on site-specific cleavage of the mRNA transcript. However, the ribosomes are not expected to be uniformly distributed on the mRNA template. The detailed spatial distribution of the ribosomes on the mRNA template can be obtained by the most recent technique, called *ribosome profiling* [150–152]. This technique effectively provides a “snapshot” of the ongoing translation by the actively engaged ribosomes on the mRNA template. There are three major steps in this method: (i) The ribosomes are first “frozen” at their instantaneous positions; (ii) the exposed parts of the mRNA transcripts (i.e., those segments not covered by any ribosome) are digested by RNase enzymes and, thereafter, the small ribosome “footprints” (segments protected by the ribosomes against the RNases) are collected separately; (iii) Finally, the ribosome-protected mRNA fragments thus collected are converted into DNA which are then sequenced. “Aligning” these footprints to the genome reveals the positions of the ribosomes at the instant when they were suddenly frozen.

Almost all the theoretical models of ribosome traffic represent the mRNA as a one-dimensional lattice where each of the L sites corresponds to a single codon. Since an individual ribosome is much larger than a single codon, each ribosome is represented by a hard rod that can cover ℓ successive codons ($\ell > 1$) simultaneously. Therefore, for the convenience of modeling, the mRNA template of L codons can be represented by a one-dimensional lattice of $L + \ell - 1$ sites where the first L sites from the left represent the L codons; the first and the L -th sites correspond to the start and stop codons, respectively. The position of a ribosome is denoted by the leftmost site of the lattice covered by it. Thus, a ribosome located at the i -th site covers all the ℓ sites from i to $i + \ell - 1$.

In this approach, ribosome traffic is treated as a problem of non-equilibrium statistical mechanics of a system of interacting “self-driven” hard rods on a one-dimensional lattice. Moreover, in these models the inter-ribosome interactions are captured through hard-core mutual exclusion principle: none of codons can be covered simultaneously by more than one ribosome. Thus, these models of ribosome traffic are essentially TASEP for hard rods: a ribosome hops forward, by one codon, with probability q per unit time, if and only if the hop does not lead to any violation of the mutual exclusion principle. Since no backtracking of ribosome has been observed, total asymmetry of hopping of the ribosomes in the TASEP-type models is justified. In TASEP-type models of ribosome traffic, all the details of the mechano-chemical cycle of a ribosome during the elongation stage is captured by a single parameter q . These models have been reviewed very recently from the perspective of statistical physics [153]. Another recent review article has summarized mathematical models of ribosome movement and translation [154]. Therefore, we’ll not discuss these in any further detail here. However, it is worth emphasizing that, strictly speaking, a ribosome is neither just a particle nor merely a hard rod; it can exist in more than one “internal” states that correspond to its various “chemical”

states. Only a few attempts have been made in recent years to capture the detailed mechano-chemistry of individual ribosomes in the quantitative models of interacting ribosomes in traffic-like situations. Chowdhury and collaborators have developed kinetic models that incorporate both the single-ribosome mechano-chemical kinetics as well as their steric interactions [137, 155, 156]. The spatio-temporal organization of the ribosomes is characterized by the average number density and average flux in the steady state. Based on the quantities, Chowdhury and coworkers have plotted the dynamic phase diagrams for ribosome traffic in spaces spanned by experimentally accessible parameters. It may become possible to test these phase diagrams in near future using the ribosome profiling technique [150–152] (or, its newer versions).

IX. COMPARISON WITH SOME OTHER MACHINES

A. Comparison with non-ribosomal peptide synthesizing machines

The monomeric subunits of non-ribosomal peptides and polyketides are amino acid and carboxylic acid, respectively. These two are the major families of natural products. Because of their importance in pharmaceutical and agrochemical industries, these natural products are the focus of attention of many leading labs [157]. A common feature of their synthesis [158–162] is that the non-ribosomal peptide synthetases (NRPS) (see fig.18) and the polyketide synthases (PKS) (see fig.19) are both large proteins which contain repeated “modules”. Each module, in turn, consists of more than one “domain” each of which has a specific activity. Each module performs one complete cycle of elongation of the polypeptide or polyketide chain. Thus, the length of the chain produced by such a machine depends on the number of modules on the machine. The operations of the NRPS and PKS resemble that of an assembly-line [163].

The modularity of the fatty acid synthase (FAS) [164] (see fig.20) and its mechanism of chain elongation has similarities with those of PKS [165–169]. The structural investigations explore not only the structure at the level of single domains, but also on the intra-module connections of the domains as well as the inter-module connections [170].

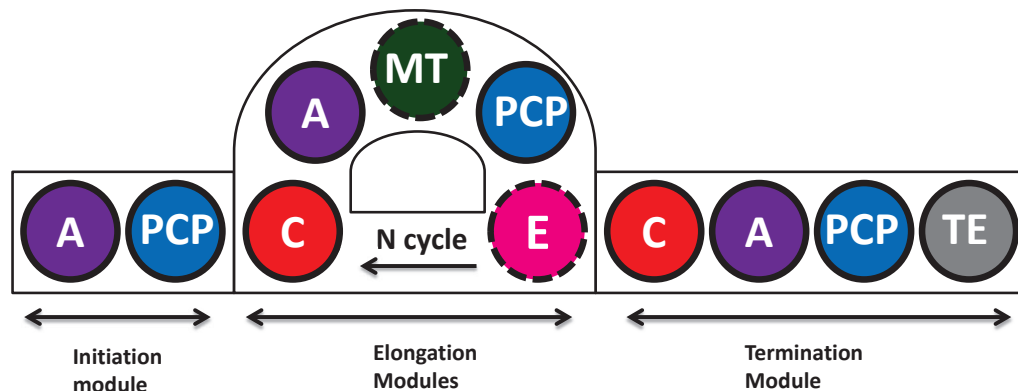


FIG. 18: Schematic representations of the chemical reaction involved in the synthesis of non ribosomal protein synthesis (adapted from [171]). Condensation (C), adenylation (A) and peptidyl carrier (PCP) are the essential domains for the non ribosomal polypeptide elongation. The reaction starts when A domain activates the amino acid by consuming an ATP molecule and produces aminoacyl adenylate. This aminoacyl reacts with the thiol group, attached with PCP domain and the C domain allows the formation of peptide bond between the aminoacyl thioester group of the growing polypeptide chain of the last module with the aminoacyl thioester group of the current module. Apart from these essential domains, some module also contain the Methyltransferase (MT) and epimerisation (E) domain which are responsible for extra enzymatic activities. MT is responsible for the methylation of the nitrogen of the amine whereas E domain cause the racemisation of the $C\alpha$ of the amino acid. The initiation module contain only A and PCP domain while the termination module includes one more extra TE domain, which cleaves the fully elongated polypeptide from PCP domain.

NRPS-mediated polypeptide synthesis does not use mRNA as a template. Instead, the identity and the order of the protein domains of the synthetase serve as the template [161, 174]. In each module of a NRPS one (or two) of the leading domains serve as “gate-keeper” and specifies the identity of the monomer to be selected. Thus, in contrast to polynucleotide templates discussed in the preceeding sections, proteins serve as the templates for NRPS-mediated polymerization. The substrate specificity of NRPS and PKS raises questions which are similar to those addressed earlier in the context of ribosomal polypeptide synthesis, namely, the mechanisms of proofreading, error tolerance



FIG. 19: Modules and domains involved in polyketide (6-deoxyerythronolide B synthase) biosynthesis (adapted from [172]). Ketosynthase (KS), acyl transferase (AT), and acyl carrier protein (ACP) are the minimal domains required in each module for the chain elongation whereas ketoreductase (KR), dehydratase (DH), and enoyl reductase (ER) are the reductive domains and required for different type of condensations.

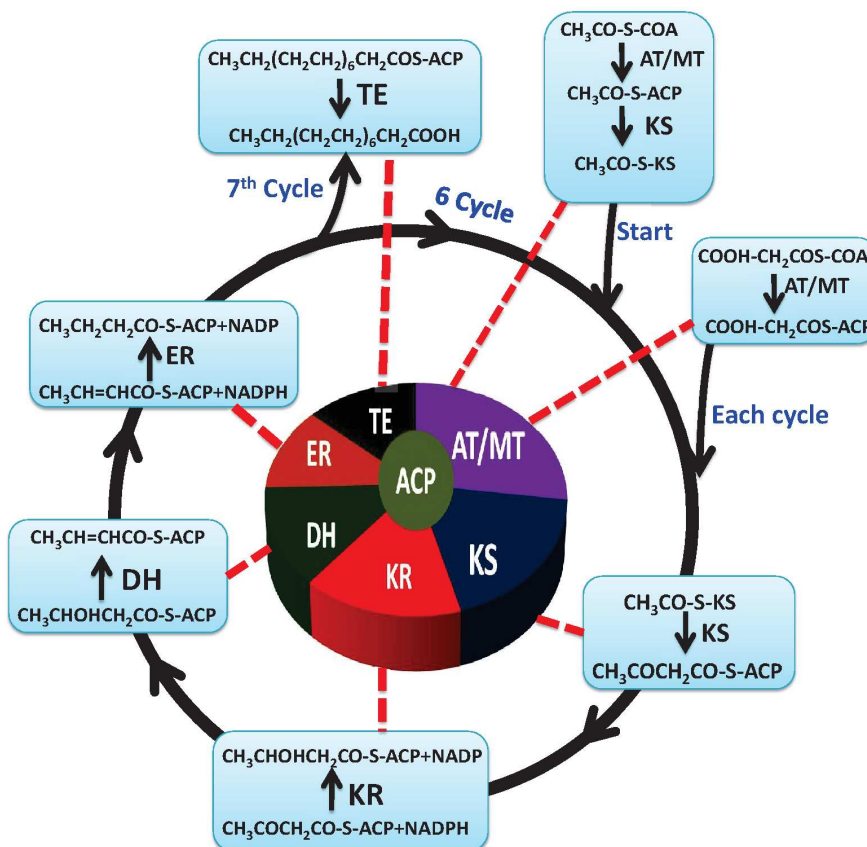


FIG. 20: Schematic representations of the chemical reactions involved in the synthesis of palmitate by FAS (adapted from [173]). Reaction starts when an acetyl group along with its coenzyme A is handed over to acyl carrier protein (ACP) by the action of acetyl/malonyl transacylase (MT/AT), from there it's transferred to β -ketoacyl synthase (KS) and reacts with a malonyl group already attached with ACP. This reaction results in the condensation of the acetyl group. Now this keto group is converted to the fully saturated carbon chain by the consecutive activities of β -ketoacyl reductase (KR), β -hydroxy-acyl dehydratase (DH) and enoyl reductase (ER). After the 7th cycle of reaction ACP is released by thioesterase (TE).

and the fidelity of the process [175, 176]. Just like in ribosomal polypeptide synthesis, one can identify three stages, namely, initiation, chain elongation and termination also in the synthesis of non-ribosomal peptides. An approximate correspondence between a ribosome and a NRPS may help in comparing the structure and function of these two types of machines [177, 178]. (i) In ribosomal synthesis, the aa-tRNA synthetase first selects the cognate amino acid and loads it onto the corresponding tRNA thereby charging it as an amino-acyl tRNA. Similarly, the A-domain of the NRPS selects the cognate amino acid and activates it as amino-acyl adenylate. (ii) The transfer of the amino-acid carrier, i.e., aa-tRNA, to the P site is assisted by the GTP hydrolysis catalyzed by the enzyme EF-Tu. The analogous

process in the NRPS is the handing over of the activated amino acid to the peptidyl carrier protein (PCP) that transfers it to the C-domain. (iii) Just as the peptidyl transferase enzyme catalyzes the peptide bond formation on the ribosome, the C-domain of the NRPS catalyzes the peptide bond formation in the non-ribosomal pathway.

B. Comparison between polynucleotide polymerases and cytoskeletal motors

Let us compare these polymerase motors with the cytoskeletal motors. (i) Polymerase motors generate forces which are about 3 to 6 times stronger than that generated by cytoskeletal motors. (ii) The step size of a polymerase is about 0.34 nm whereas that of a kinesin is about 8 nm. (iii) The polymerase motors are slower than the cytoskeletal motors by two orders of magnitude. (iv) Natural nucleic acid tracks are intrinsically inhomogeneous because of the inhomogeneity of nucleotide sequences whereas the cytoskeletal tracks are homogeneous and exhibit perfect periodic order.

C. Polymerases as “tape-copying Turing machines”: dissipationless computation

Template-directed polymerization has been analyzed in terms of the principles of information theory. The pioneering works were carried out by Wolkenshtein and Eliasevich [179] and by Davis [180]. These authors calculated the lowering of entropy, i.e., generation of information, in template-directed polymerization. These initial calculations were based on the simplifying assumption that each nucleotide addition is an event independent of that of the neighboring ones on the same template. In a recent work Arias-Gonzalez [181] has extended these theories by incorporating the effect of interactions between the neighboring nucleotides. However, Arias-Gonzalez [181] assumed an equilibrium pathway for the process which implies absence of dissipation. Obviously, this is not valid for any real template-directed polymerization process. Effects of the nonequilibrium conditions of template-directed polymerization processes on the resulting information transmission were investigated by Andrieux and Gaspard [182, 183].

A Turing machine carries out computation by repeating a cycle of logical operations. In each cycle it reads input information from a digital tape and, then, produces an output based on a set of rules. The translocation of a RNA polymerase along its template resembles a Turing machine in the sense that it also moves along a digital tape (DNA), reads information from it, and produces an output as a result of its “computation” based on its “rules”. However, the output, namely the RNA, is another digital tape. Therefore, a RNAP (and, similarly, a ribosome) can be regarded as a “tape-copying Turing machine” [184] that polymerizes its output tape, instead of merely writing on a pre-synthesized tape [8].

Polymerization of RNA by RNAP has been analyzed also by Mooney et al. [185] from the perspective of information processing. Unlike the digital logic of a computer, decisions made by a polymerase are governed by competing rates and equilibria among alternative conformations and complexes. The changes in these conformations, i.e., the regulatory decisions made by a RNAP depend on two types of information input (to be distinguished from energy input): (i) intrinsic, and (ii) extrinsic. The intrinsic input include, for example, (a) the segment of the DNA template within the transcription bubble, (b) the nascent RNA, etc. whereas all the transcription factors are extrinsic inputs. Depending on the regulatory decisions made by the RNAP, it either elongates the RNA or pauses, or backtracks. Although futile cycles cause dissipation, these are essential for error correction. Dissipationless operation of these machines is possible only if every step is error-free which, in turn, is achievable in the vanishingly small speed, i.e., reversible limit [9]. In other words, a polymerase is a Maxwell’s demon that “accumulates and stores” information by creating an ordered sequence of nucleotides, as directed by the corresponding template [186].

X. SUMMARY AND CONCLUSION

In this article we have reviewed some of the recent progress in understanding the common features of template-directed polymerization. We have discussed the structural features of the machines and the kinetic processes that they drive. Each faces conflicting requirements of speed and fidelity of polymerization. These tape-copying Turing machines hold promise for physical realization of dissipationless computation in future. We have also drawn attention to another class of modular machines which also carry out an altogether different type of template-directed polymerization. Such natural machines in living systems have already inspired designing of artificial “molecular assembly line” [163]. We hope theoretical models would be developed for these modular machines in near future for making quantitative characterization of their operational mechanism. Finally, fundamental questions on the constraints imposed by the “local detailed-balance conditions” on the rates of the various motor-driven processes [187] need to be addressed in the context of template-directed polymerization.

Acknowledgements: One of the authors (DC) thanks Ashok Garai and Tripti Tripathi for many discussions on the topic of this review and for enjoyable collaborations. This work has been supported at IIT Kanpur by the Dr. Jag Mohan Garg Chair professorship (DC) and a CSIR fellowship (AKS). It has also been supported, in part, at the Ohio State University, Columbus, by the Mathematical Biosciences Institute and the National Science Foundation under grant DMS 0931642.

-
- [1] J. Frank, *Molecular machines in biology: workshop of the cell* (Cambridge University Press, 2011).
 - [2] E. Shapiro and Y. Benenson, *Bringing DNA computers to life*, Sci. Am. 45-51 (May, 2006).
 - [3] V.A. Erdmann and J. Barciszewski, *2011: 50th anniversary of the discovery of the genetic code*, Angew. Chem. Int. Ed. **50**, 9546-9552 (2011).
 - [4] J. M. Ogle and V. Ramakrishnan, *Structural insight into translational fidelity*, Annu. Rev. Biochem. **74**, 129177 (2005).
 - [5] H. S. Zaher and R. Green, *Fidelity at the molecular level: lessons from protein synthesis*, Cell **136**, 746762 (2009).
 - [6] J.F. Sydow and P. Cramer, *RNA polymerase fidelity and transcriptional proofreading*, Curr. Opinion Struct. Biol. **19**, 732739 (2009).
 - [7] T.A. Kunkel and K. Bebenek, *DNA replication fidelity*, Annu. Rev. Biochem. **69**, 497-529 (2000).
 - [8] C. H. Bennett, *The thermodynamics of computation- a review*, Int. J. Theor. Phys. **21**, 905-940 (1982).
 - [9] C. H. Bennett, *Dissipation-error tradeoff in proofreading*, Biosystems **11**, 85-91 (1979).
 - [10] C.H. Bennett and M. Donkor, *Thermodynamics of error correction: speed-error-dissipation tradeoff in copying*, Information Theory Workshop (IEEE, 2008).
 - [11] K. H. Choi, *Viral polymerases*, in: *Viral molecular machines*, eds. M.G. Rossmann and V.B. Rao, Adv. Expt. Med. Biol. **726**, 267-304 (2012).
 - [12] R. Lipowsky, S. Klumpp, and T. M. Nieuwenhuizen, *Random walks of cytoskeletal motors in open and closed compartments*, Phys. Rev. Lett. **87**, 108101 (2001).
 - [13] A. Parmeggiani, T. Franosch and E. Frey, *Phase coexistence in driven one-dimensional transport*, Phys. Rev. Lett. **90**, 086601 (2003).
 - [14] M.R. Evans, R. Juhasz and L. Santen, *Shock formation in an exclusion process with creation and annihilation*, Phys. Rev. E **68**, 026117 (2003).
 - [15] V. Popkov, A. Rakos, R.D. Williams, A.B. Kolomeisky and G.M. Schütz, *Localization of shocks in driven diffusive systems without particle number conservation*, Phys. Rev. E **67**, 066117 (2003).
 - [16] R. Lipowsky and S. Klumpp, *'Life is motion': multiscale motility of molecular motors*, Physica A **352**, 53-112 (2005).
 - [17] R. Lipowsky, Y. Chai, S. Klumpp, S. Liepelt and M.J.I. Müller, *Molecular motor traffic: from biological nanomachines to macroscopic transport*, Physica A **372**, 34-51 (2006).
 - [18] J. Gelles and R. Landick, *RNA polymerase as a molecular motor*, Cell, **93**, 13-16 (1998).
 - [19] L. Bai, R.M. Fulbright and M.D. Wang, *Mechano-chemical kinetics of transcription elongation*, Phys. Rev. Lett. **98**, 068103 (2007).
 - [20] R. Sousa, *Machinations of a Maxwellian Demon*, Cell **120**, 155-158 (2005).
 - [21] Q. Guo and R. Sousa, *Translocation by T7 RNA polymerase: a sensitively poised Brownian ratchet*, J. Mol. Biol. **358**, 241-254 (2006).
 - [22] E.A. Abbondanzieri, W.J. Greenleaf, J. W. Shaevitz, R. Landick and S.M. Block, *Direct observation of base-pair stepping by RNA polymerase*, Nature, **438**, 460-465 (2005).
 - [23] P. Cramer, K.J. Armache, S. Baumli, S. Benkert, F. Brueckner, C. Buchen, G.E. Damshma, S. Dengl, S.R. Geiger, A.J. Jasiak, A. Jawhari, S. Jennebach, T. Kamenski, H. Kettenberger, C.D. Kuhn, E. Lehmann, K. Leike, J.F. Sydow and A. Vannini, *Structure of eukaryotic RNA polymerases*, Annu. Rev. Biophys. **37**, 337-352 (2008).
 - [24] G. Bar-Nahum, V. Epshtein, A.E. Ruckenstein, R. Rafikov, A. Mustaev and E. Nudler, *A ratchet mechanism of transcription elongation and control*, Cell **120**, 183-193 (2005).
 - [25] J. Yu and G. Oster, *A small post-translocation energy bias aids nucleotide selection in T7 RNA polymerase transcription*, Biophys. J. **102**, 532-541 (2012).
 - [26] T. Tripathi and D. Chowdhury, *Interacting RNA polymerase motors on a DNA track: effects of traffic congestion and intrinsic noise on RNA synthesis*, Phys. Rev. E **77**, 011921 (2008).
 - [27] Y. R. Yamada and C. S. Peskin, *A look-ahead model for the elongation dynamics of transcription*, Biophys. J. **96**, 30153031 (2009).
 - [28] Y. R. Yamada and C. S. Peskin, *The influence of look-ahead on the error rate of transcription.*, Math. Model. Nat. Phenom. **27**, 206-227 (2010).
 - [29] T. Tripathi, G. M. Schutz and D. Chowdhury, *RNA polymerase motors: dwell time distribution, velocity and dynamical phases* J. Stat. Mech. Theor. Exp. **P08018** (2009).
 - [30] R. Landick, *A long time in the making- the nobel prize for RNA polymerase*, Cell **127**, 1087-1090 (2006).
 - [31] J. W. Shaevitz, E. A. Abbondanzieri, R. Landick. and S. M. Block, *Backtracking by single RNA polymerase molecules observed at near-base-pair resolution*, Nature **426**, 684-687 (2003).
 - [32] E.A. Galburt, S.W. Grill, A. Wiedmann, L. Lubkowska, J. Choy, E. Nogales, M. Kashlev and C. Bustamante, *Backtracking determines the force sensitivity of RNAPII in a factor-dependent manner*, Nature **446**, 820-823 (2007).

- [33] L. Bai, A. Shundrovsky and M.D. Wang, *Sequence-dependent kinetic model for transcription elongation by RNA polymerase*, J. Mol. Biol. **344**, 335-349 (2004).
- [34] R. Landick, *Transcriptional pausing without backtracking*, Proc. Natl. Acad. Sci. **106**, 8797-8798 (2009).
- [35] R. V. Dalal, M. H. Larson, K. C. Neuman, J. Gelles, R. Landick, and S. M. Block, *Pulling on the nascent RNA during transcription does not alter kinetics of elongation or ubiquitous pausing*, Molecular Cell **23**, 231-239 (2006).
- [36] M. Voliotis, N. Cohen, C. Molina-Paris and T.B. Liverpool, *Fluctuations, pauses, and backtracking in DNA transcription*, Biophys. J. **94**, 334-348 (2008).
- [37] Martin Depken, Eric A. Galburt and Stephan W. Grill *The Origin of Short Transcriptional Pauses* Biophys. J. **93**, 2189-2193 (2009).
- [38] Ping Xie, *A dynamic model for transcription elongation and sequence-dependent short pauses by RNA polymerase*, BioSystem **93**, 199-210 (2008).
- [39] Ping Xie, *Dynamics of backtracking long pauses of RNA polymerase*, Biochimica et Biophysica Acta (BBA) - Gene Structure and Expression **1789**, 212-219 (2009).
- [40] Ping Xie, *A dynamic model for processive transcription elongation and backtracking long pauses by multisubunit RNA polymerases*, Proteins: Structure, Function and Bioinformatics, **80**, 2020-2034 (2012).
- [41] M. Voliotis, N. Cohen, C. Molina-Pars, and T. B. Liverpool, *Backtracking and proofreading in DNA transcription*, Phys. Rev. Lett. **102**, 258101 (2009).
- [42] M. Sahoo and S. Klumpp, *Transcriptional proofreading in dense RNA polymerase traffic*, EPL **96**, 60004, (2011).
- [43] V. Epshtein and E. Nudler, *Cooperation between RNA polymerase molecules in transcription elongation*, Science **300**, 801-805 (2003).
- [44] V. Epshtein, F. Toulme, A.R. Borukhov and E. Nudler, *Transcription through roadblocks: the role of RNA polymerase cooperation*, EMBO J. **22**, 4719-4727 (2003).
- [45] E.A. Galburt, J.M.R. Parrondo and S.W. Grill, *RNA polymerase pushing*, Biophys. Chem. **157**, 43-47 (2011).
- [46] H. Saeki and J. Q. Svejstrup, *Stability, flexibility, and dynamic interactions of colliding RNA polymerase II elongation complexes*, Mol. Cell **35**, 191-205 (2009).
- [47] K. Sneppen, I. B. Dodd, K. E. Shearwin, A. C. Palmer, R. A. Schubert, B. P. Callen, J. B. Egan *A mathematical model for transcriptional interference by RNA polymerase traffic in Escherichia coli*, J. Mol. Biol. **346**, 399409 (2005).
- [48] S. Klumpp and T. Hwa, *Growth-rate-dependent partitioning of RNA polymerases in bacteria*, Proc. Natl. Acad. Sci. USA, **105**, 20245-20250 (2008).
- [49] Yoshihiro Ohta, Tatsuhiko Kodama, and Sigeo Ihara, *Cellular-automaton model of the cooperative dynamics of RNA polymerase II during transcription in human cells*, Phys. Rev. E **84**, 041922 (2011).
- [50] Gijs J.L. Wuite, Steven B. Smith, Mark Young, David Keller and Carlos Bustamante, *Single-molecule studies of the effect of template tension on T7 DNA polymerase activity*, Nature **404**, 103-106 (2000).
- [51] B. Maier, D. Bensimon and V. Croquette, *Replication by a single DNA polymerase of a stretched single-stranded DNA*, Proc. Natl. Acad. Sci. USA **97**, 12002-12007 (2000).
- [52] A. Goel, M.D. Frank-Kamenetskii, T. Ellenberger and D. Herschbach, *Tuning DNA "strings": modulating the rate of DNA replication with mechanical tension*, Proc. Natl. Acad. Sci. USA **98**, 8485-8489 (2001).
- [53] A. Goel, R.D. Astumian and D. Herschbach, *Tuning and switching a DNA polymerase motor with mechanical tension*, Proc. Natl. Acad. Sci. USA **100**, 9699-9704 (2003).
- [54] I. Andricioaei, A. Goel, D. Herschbach and M. Karplus, *Dependence of DNA polymerase replication rate on external forces: a model based on molecular dynamics simulations*, Biophys. J. **87**, 1478-1497 (2004).
- [55] L. J. Reha-Krantz *DNA polymerase proofreading: Multiple roles maintain genome stability.*, Biochim. Biophys. Acta. **1804**, 1049-1063 (2010).
- [56] B. Ibarra, Y. R. Chemla, S. Plyasunov, S. B. Smith, J. M. Lzaro, M. Salas and C Bustamante, *Proofreading dynamics of a processive DNA polymerase*, EMBO J. **28**, 2794-2802 (2009).
- [57] A. R. Fersht, J. W. Knill-Jones, W.C. Tsui, *Kinetic basis of spontaneous mutation: Misinsertion frequencies, proofreading specificities and cost of proofreading by DNA polymerases of Escherichia coli*, J. Mol. Biol. **156**, 37-51 (1982).
- [58] A. K. Sharma and D. Chowdhury, *Error correction during DNA replication*, Phys. Rev. E **86**, 011913 (2012).
- [59] Kenneth A. Johnson, *The kinetic and chemical mechanism of high-fidelity DNA polymerases*, Biochimica et Biophysica Acta **1804**, 10411048 (2010).
- [60] Linda B. Bloom and Myron F. Goodman, *A sliding clamp monkey wrench*, Nat. Struct. Biol. **8**, 829-831 (2001).
- [61] Linda B. Bloom, *Dynamics of loading the Escherichia coli DNA polymerase processivity clamp*, Crit. Rev. Biochem. and Mol. Biol. **41**, 179-208 (2006).
- [62] D. Jeruzalmi, M. O'Donnell, and J. Kuriyan, *Clamp loaders and sliding clamps*, Curr. Opin. Struct. Biol. **12**, 217-224 (2002).
- [63] C. Indiani and M. O'Donnell, *The replication clamp-loading machine at work in the three domains of life*, Nat. Rev. Mol. Cell Biol. **7**, 751-761 (2006).
- [64] V. Ellison and B. Stillman, *Opening of the clamp*, Cell **106**, 655-660 (2001).
- [65] D. Barsky and C. Venclovas, *DNA sliding clamps: just the right twist to load onto DNA*. Curr. Biol. **15**, R989-R992 (2005).
- [66] D.N. Frick and C.C. Richardson, *DNA primases*, Annu Rev. Biochem. **70**, 39-80 (2001).
- [67] T.A. Baker and S.P. Bell, *Polymerases and the replisome: machines within machines*, Cell, **92**, 295-305 (1998).
- [68] S.J. Benkovic, A.M. Valentine and F. Salinas, *Replisome-mediated DNA replication*, Annu. Rev. Biochem. **70**, 181-208 (2001).

- [69] A. Johnson and M. O'Donnel, *Cellular DNA replicases: components and dynamics at the replication fork*, Annu. Rev. Biochem. **74**, 283-315 (2005).
- [70] M.J. Davey and M. O'Donnel, *Mechanism of DNA replication*, Curr. Opin. Chem. Biol. **4**, 581-586 (2000).
- [71] I. Frouin, A. Montecucco, S. Spadari and G. Maga, *DNA replication: a complex matter*, EMBO Rep. **4**, 666-670 (2003).
- [72] D.R. Herendeen and T.J. Kelley, *DNA polymerase III: running rings around the fork*, Cell, **84**, 5-8 (1996).
- [73] P. Thömmes and U. Hübscher, *Eukaryotic DNA replication*, Eur. J. Biochem. **194**, 699-712 (1990).
- [74] S.P. Bell and A. Dutta, *DNA replication in eukaryotic cells*, Annu. Rev. Biochem. **71**, 333-374 (2002).
- [75] P. Garg and P.M.J. Burgers, *DNA polymerases that propagate the eukaryotic DNA replication fork*, Crit. Rev. Biochem. and Mol. Biol. **40**, 115-128 (2005).
- [76] E.R. Barry and S.D. Bell, *DNA replication in the archaea*, Microbiol. and Mol. Biol. Rev. **70**, 876-887 (2006).
- [77] A.T. McGeoch and S.D. Bell, *Extra-chromosomal elements and the evolution of cellular DNA replication machineries*, Nat. Rev. Mol. Cell Biol. **9**, 569-574 (2008).
- [78] A.M. van Oijen and J. J. Loparo, *Single-molecule studies of the replisome*, Annu. Rev. Biophys. **39**, 429-448 (2010).
- [79] S.K. Perumal, H. Yue, M.M. Spiering and S.J. Benkovic, *Single-molecule studies of DNA replisome function*, Biochim. Biophys. Acta - proteins & proteomics **1804**, 1094-1112 (2010).
- [80] S.S. Patel, M. Pandey and D. Nandakumar, *Dynamic coupling between the motors of DNA replication: hexameric helicase, DNA polymerase, and primase*, Curr. Opin. Chem. Biol. **15**, 595-605 (2011).
- [81] J.B. Lee, R.K. Hite, S.M. Hamdan, X. Sunney Xie, C.C. Richardson and A.M. van Oijen, *DNA primase acts as a molecular brake in DNA replication*, Nature, **439**, 621-624 (2006).
- [82] S.J. Lee, B. Zhu, S.M. Hamdan and C.C. Richardson, *Mechanism of sequence-specific template binding by the DNA primase of bacteriophage T7*, Nucl. Acids Res. **38**, 4372-4383 (2010).
- [83] T. Blumenthal and G.G. Carmichael, *RNA replication: function and structure of Q β -replicase*, Annu. Rev. Biochem. **48**, 525-548 (1979).
- [84] J. Ortin and F. Parra, *Structure and function of RNA replication*, Annu. Rev. Microbiol. **60**, 305-326 (2006).
- [85] K.K.S. Ng, J.J. Arnold and C.E. Cameron, *Structure- function relationships among RNA-dependent RNA polymerases*, Curr. Top. Microbiol. Immunol. **320**, 137-156 (2008).
- [86] P. Roy, *Bluetongue virus: dissection of the polymerase complex*, J. Gen. Virology **89**, 1789-1804 (2008).
- [87] C. Ferrer-Orta, A. Arias, C. Escarmis and N. Verdager, *A comparison of viral RNA-dependent RNA polymerases*, Curr. Opin. Struct. Biol. **16**, 27-34 (2006).
- [88] A. A. van Dijk, E. V. Makeyev and D. H. Bamford, *Initiation of viral RNA-dependent RNA polymerization*, Journal of General Virology, **85**, 1077-1093 (2004).
- [89] N. J. Dimmock, A. J. Easton and K. N. Leppard, *Introduction to modern virology* (Blackwell publishing, 2007).
- [90] Romn Galetto and Matteo Negroni *Retroviruses*, in: *Viral Genome replication*, eds. C.E. Cameron et al. 109-128 (Springer, 2009).
- [91] M. Wendeler, J.T. Miller and S.F.J. Le Grice, *Human immunodeficiency virus reverse transcriptase*, in: *Viral genome replication*, eds. C.E. Cameron et al. (Springer, 2009).
- [92] A. Hizi and A. Herschhorn, *Retroviral reverse transcriptase (other than those of HIV-1 and murine leukemia virus): a comparison of their molecular and biochemical properties*, Virus Res. **134**, 203-220 (2008).
- [93] A. Herschhorn and A. Hizi, *Retroviral reverse transcriptase*, Cell. Mol. Life Sci. **67**, 2717-2747 (2010).
- [94] Greg L. Beilhartz and Matthias Götte *HIV-1 ribonuclease H: structure, catalytic mechanism and inhibitors*, Viruses **2**, 900-926 (2010).
- [95] Elio A. Abbondanzieri et al. *Dynamic binding orientations direct activity of HIV reverse transcriptase*, Nature **453**, 184-189 (2008).
- [96] H.L. Levin, *It's prime time for reverse transcriptase*, Cell **88**, 5-8 (1997).
- [97] Louis M. Mansky, *Retrovirus mutation rates and their role in genetic variation*, J. Gen. Virology, **79**, 1337-1345 (1998).
- [98] A.K. Sharma and D. Chowdhury (to be published).
- [99] M. Elas-Arnanz and M. Salas, *Bacteriophage phi29 DNA replication arrest caused by codirectional collisions with the transcription machinery*, The EMBO Journal **16**, 5775-5783 (1997).
- [100] M. Elas-Arnanz and M. Salas, *Resolution of head-on collisions between the transcription machinery and bacteriophage Φ 29 DNA polymerase is dependent on RNA polymerase translocation*, The EMBO J. **18**, 5675-5682 (1999).
- [101] P. Soutanas, *The replication-transcription conflict*, Transcription **2**, 140-144 (2011).
- [102] A.S. Spirin, *Ribosomes*, (Kluwer Academic/Plenum, 1999).
- [103] A.S. Spirin, *Ribosome as a molecular machine*, FEBS Lett. **514**, 2-10 (2002).
- [104] A.S. Spirin, *The ribosome as an RNA-based molecular machine*, RNA Biology **1**, 3-9 (2004).
- [105] A.S. Spirin, *The ribosome as a conveying thermal ratchet machine*, J. Biol. Chem. **284**, 21103-21119 (2009).
- [106] K.Y. Sanbonmatsu, *Computational studies of molecular machines: the ribosome*, Curr. Opin. Struct. Biol. **22**, 168-174 (2012).
- [107] K. Abel and F. Jurnak, *A complex profile of protein elongation: translating chemical energy into molecular movement*, Structure **4**, 229-238 (1996).
- [108] J. Ling, N. Reynolds and M. Ibba, *Aminoacyl-tRNA synthesis and translational quality control*, Annu. Rev. Microbiol. **63**, 61-78 (2009).
- [109] C.S. Francklyn, *DNA polymerases and aminoacyl-tRNA synthetases: shared mechanisms for ensuring fidelity of gene expression*, Biochem. **47**, 11695-11703 (2008).
- [110] E. Westhof and N. Leontis, *Atomic glimpses on a billion-year-old molecular machine*, Angew. Chem. Int. Ed. **39**, 1587-1591

- (2000).
- [111] P.B. Moore and T.A. Steitz, *The structural basis of large ribosomal subunit function*, Annu. Rev. Biochem. **72**, 813-850 (2003).
 - [112] T. A. Steitz, *A structural understanding of the dynamic ribosome machine*, Nat. Rev. Mol. Cell Biol. **9**, 242-253 (2008).
 - [113] T.A. Steitz, *From the structure and function of the ribosome to new antibiotics (Nobel Lecture)*, Angewandte Chemie International Ed. **49**, 4381-4398 (2010).
 - [114] A. Yonath, *The search and its outcome: high-resolution structures of ribosomal particles from mesophilic, thermophilic, and halophilic bacteria at various functional states*, Annu. Rev. Biophys. & Biomol. Struct. **31**, 257-273 (2002).
 - [115] A. Yonath, *Hibernating bears, antibiotics, and evolving ribosome (Nobel lecture)*, Angewandte Chemie International Ed. **49**, 4340-4354 (2010).
 - [116] V. Ramakrishnan, *Ribosome structure and the mechanism of translation*, Cell **108**, 557-572 (2002).
 - [117] T.M. Schmering and V. Ramakrishnan, *What recent ribosome structure have revealed about the mechanism of translation*, Nature **461**, 1234-1242 (2009).
 - [118] V. Ramakrishnan, *Unraveling the structure of the ribosome (Nobel Lecture)*, Angewandte Chemie International Ed. **49**, 4355-4380 (2010).
 - [119] J. Frank, *The ribosome- a macromolecular machine par excellence*, Chem. & Biol. **7**, R133-R141 (2000).
 - [120] X. Agirrezabala and J. Frank, *Elongation in translation as a dynamic interaction among the ribosome, tRNA, and elongation factors EF-G and EF-Tu*, Quart. Rev. Biophys. **42**, 159-200 (2009).
 - [121] J. Frank and R. L. Gonzales, *Structure and dynamics of a processive Brownian motor: the translating ribosome*, Annu. Rev. Biochem. **79**, 381-412 (2010).
 - [122] M.M. Yusupov, G.Z. Yusupova, A. Baucom, K. Lieberman, T.N. Earnest, J.H.D. cate and H.F. Noller, *Crystal structure of the ribosome at 5.5Å⁰ resolution*, Science **292**, 883-896 (2001).
 - [123] G. Blaha and P. Ivanov, *Structure of the ribosome*, in: *Protein synthesis and ribosome structure*, eds. K.H. Nierhaus and D.N. Wilson (Wiley-VCH, 2004).
 - [124] R.A. Marshall, C.E. Aitken, M. Dorywalska and J.D. Puglisi, *Translation at the single-molecule level*, Annu. Rev. Biochem. **77**, 177-203 (2008).
 - [125] S. Blanchard, R.L. Gonzalez Jr., H.D. Kim, S. Chu and J.D. Puglisi, *tRNA selection and kinetic proofreading in translation*, Nat. Str. & Mol. Biol. **11**, 1008-1014 (2004).
 - [126] S. Uemura, M. Dorywalska, T.H. Lee, H.D. Kim, J.D. Puglisi and S. Chu, *Peptide bond formation destabilizes Shine-Dalgarno interaction on the ribosome*, Nature **446**, 454-457 (2007).
 - [127] J.B. Munro, A. Vaiana, K.Y. Sanbonmatsu and S.C. Blanchard, *A new view of protein synthesis: mapping the free energy landscape of the ribosome using single-molecule FRET*, Biopolymers **89**, 565-577 (2008).
 - [128] J. B. Munro, K. Y. Sanbonmatsu, C.M.T. Spahn and S.C. Blanchard, *Navigating the ribosome's metastable energy landscape*, Trends in Biochem. Sci. **34**, 390-400 (2009).
 - [129] S.C. Blanchard, *Single-molecule observations of ribosome function*, Curr. Opin. Struct. Biol. **19**, 103-109 (2009).
 - [130] S. Uemura, C. E. Aitken, J. Korlach, B.A. Flusberg, S. W. Turner and J.D. Puglisi, *Real-time tRNA transit on single translating ribosome at codon resolution*, Nature **464**, 1012-1017 (2010).
 - [131] C. E. Aitken and J. D. Puglisi, *Following the intersubunit conformation of the ribosome during translation in real time*, Nat. Struct. Mol. Biol. **17**, 793-800 (2010).
 - [132] F. Vanzi, S. Vladimirov, C.R. Knudsen, Y.E. Goldman and B.S. Cooperman, *Protein synthesis by single ribosomes*, RNA, **9**, 1174-1179 (2003).
 - [133] Y. Wang, H. Qin, R.D. Kudaravalli, S.V. Kirillov, G.T. Dempsey, D. Pan, B.S. Cooperman and Y.E. Goldman, *Single-molecule structural dynamics of EF-G-ribosome interaction during translocation*, Biochemistry **46**, 10767-10775 (2007).
 - [134] J.D. Wen, L. Lancaster, C. Hodges, A.C. Zeri, S.H. Yoshimura, H.F. Noller, C. Bustamante and I. Tinoco Jr., *Following translation by single ribosome one codon at a time* Nature **452**, 598-603 (2008).
 - [135] I. Tinoco Jr. and J. D. Wen, *Simulation and analysis of single-ribosome translation*, Phys. Biol. **6**, 025006 (2009).
 - [136] J.R. Buchan and I. Stansfield, *Halting a cellular production line: responses to ribosomal pausing during translation*, Biol. Cell **99**, 475-487 (2007).
 - [137] A. Garai, D. Chowdhury, D. Chowdhury and T.V. Ramakrishnan, *Stochastic kinetics of ribosomes: Single motor properties and collective behavior*, Phys. Rev. E **80**, 011908 (2009).
 - [138] A. K. Sharma and D. Chowdhury, *Distribution of dwell times of a ribosome: effects of infidelity, kinetic proofreading and ribosome crowding*, Physical Biology, **8**, 026005 (2011).
 - [139] D. Chowdhury, L. Santen and A. Schadschneider, *Statistical physics of vehicular traffic and some related systems* Phys. Rep. **329**, 199-329 (2000).
 - [140] A. Schadschneider, D. Chowdhury and K. Nishinari, *Stochastic transport in complex systems: from molecules to vehicles* (Elsevier, 2010).
 - [141] D. Chowdhury, A. Schadschneider and K. Nishinari, *Physics of Transport and Traffic Phenomena in Biology: from molecular motors and cells to organisms*, Phys. of Life Rev. **2**, 318-352 (2005).
 - [142] J.R. Warner, A. Rich and C.E. Hall, *Electron microscope studies of ribosomal clusters synthesizing hemoglobin* Science **138**, 1399-1403 (1962).
 - [143] J.R. Warner, P.M. Knopf and A. Rich, *A multiple ribosomal structure in protein synthesis*, Proc. Natl. Acad. Sci. USA **49**, 122-129 (1963).
 - [144] A. Rich, *The excitement of discovery*, Annu. Rev. Biochem. **73**, 1-37 (2004).
 - [145] H. Noll, *The discovery of polyribosomes*, Bioessays **30**, 1220-1234 (2008).

- [146] N. Mitarai, K. Sneppen and S. Pedersen, *Ribosome collisions and translation efficiency: optimization by codon usage and mRNA destabilization*, J. Mol. Biol. **382**, 236-245 (2008).
- [147] Y. Arava, Y. Wang, J.D. Storey, C.L. Liu, P.O. Brown and D. Herschlag, *Genome-wide analysis of mRNA translation profiles in *Saccharomyces cerevisiae**, Proc. Natl. Acad. Sci. USA **100**, 3889-3894 (2003).
- [148] E. Mikamo, C. Tanaka, T. Kanno, H. Akiyama, G. Jung, H. Tanaka, T. Kawai *Native polysomes of *Saccharomyces cerevisiae* in liquid solution observed by atomic force microscopy* J. Struct. Biol. **151**, 106110 (2005).
- [149] Y. Arava, F.E. Boas, P.O. Brown and D. Herschlag, *Dissecting eukaryotic translation and its control by ribosome density mapping*, Nucl. Acids Res. **33**, 2421-2432 (2005).
- [150] N.T. Ingolia, S. Ghaemmaghami, J.R.S. Newman and J.S. Weissman, *Genome-wide analysis in vivo of translation with nucleotide resolution using ribosome profiling*, Science **324**, 218-223 (2009).
- [151] H. Guo, N.T. Ingolia, J.S. Weissman and D.P. Bartel, *Mammalian microRNAs predominantly act to decrease target mRNA levels*, Nature **466**, 835-840 (2010).
- [152] N.T. Ingolia, L.F. Lareau and J.S. Weissman, *Ribosome profiling of mouse embryonic stem cells reveals the complexity and dynamics of mammalian proteomes*, Cell **147**, 789-802 (2011).
- [153] T. Chou, K. Mallick and R.K.P. Zia, *Non-equilibrium statistical mechanics: from a paradigmatic model to biological transport*, Rep. Prog. Phys. **74**, 116601 (2011).
- [154] T. von der Haar, *Mathematical and computational modelling of ribosomal movement and protein synthesis: an overview*, Comp. and Struct. Biotechnol. J. **1**, e201204002 (2012).
- [155] A. Basu and D. Chowdhury, *Traffic of interacting ribosomes: effects of single-machine mechanochemistry on protein synthesis*, Phys. Rev. E **75**, 021902 (2007).
- [156] A.K. Sharma and D. Chowdhury, *Stochastic theory of protein synthesis and polysome: ribosome profile on a single mRNA transcript*, J. Theor. Biol. **289**, 36-46 (2011).
- [157] B. Wilkinson and J. Micklefield, *Mining and engineering natural product biosynthetic pathways*, Nat. Chem. Biol. **3**, 379-386 (2007).
- [158] J.M. Crawford and C.A. Townsend, *New insights into the formation of fungal aromatic polyketides*, Nat. Rev. Microbiol. **8**, 879-889 (2010).
- [159] M.A. Marahiel, *Working outside the protein synthesis rules: insights into non-ribosomal peptide synthesis*, J. Peptide Sci. **15**, 799-807 (2009).
- [160] J. Staunton and K.J. Weissman, *Polyketide biosynthesis: a millenium review*, Nat. Prod. Rep. **18**, 380-416 (2001).
- [161] M.A. Fischbach and C.T. Walsh, *Assembly-line enzymology for polyketide and nonribosomal peptide antibiotics: logic, machinery, and mechanisms*, Chem. Rev. **106**, 3468-3496 (2006).
- [162] J.L. Meier and M.D. Burkart, *The chemical biology of modular biosynthetic enzymes*, Chem Soc. Rev. **38**, 2012-2045 (2009).
- [163] B. Chow and J.M. Jacobson, *Biologically inspired molecular assembly lines*, BT Technol. J. **22**, 270-277 (2004).
- [164] C. Khosla, S. Kapur and D.E. Cane, *Revisiting the modularity of modular polyketide synthases*, Curr. Opin. Chem. Biol. **13**, 135-143 (2009).
- [165] S.W. White, J. Zheng, Y.M. Zhang and C.O. Rock, *The structural biology of type II fatty acid biosynthesis*, Annu. Rev. Biochem. **74**, 791-831 (2005).
- [166] O. Tehlivets, K. Scheuringer and S.D. Kohlwein, *Fatty acid synthesis and elongation in yeast*, Biochim. Biophys. Acta **1771**, 255-270 (2007).
- [167] A. Jakobsson, R. Westerberg and A. Jacobsson, *Fatty acid elongases in mammals: their regulation and roles in metabolism*, Prof. Lipid Res. **45**, 237-249 (2006).
- [168] A.E. Leonard, S.L. Pereira, H. Sprecher and Y.S. Huang, *Elongation of long-chain fatty acids*, Prog. Lipid Res. **43**, 36-54 (2004).
- [169] S. Smith, A. Witkowski and A.K. Joshi, *Structural and functional organization of the animal fatty acid synthase*, Prog. Lipid Res. **42**, 289-317 (2003).
- [170] A. Koglin and C.T. Walsh, *Structural insights into nonribosomal peptide enzymatic assembly lines*, Nat. Prod. Rep. **26**, 987-1000 (2009).
- [171] G. L. Challis and J. H. Naismith, *Structural aspects of non-ribosomal peptide biosynthesis*, Current Opin. Struct. Biol. **14**, 748756 (2004).
- [172] D. Bedford, J. R. Jacobsen, G. Luo, D. E. Cane and C. Khosla, *A functional chimeric modular polyketide synthase generated via domain replacement*, Chemistry & Biology **3**, 827-831 (1996).
- [173] S. S. Chirala and S. J. Wakil, *Structure and Function of Animal Fatty Acid Synthase*, Lipids **39**, 1045-1053 (2004).
- [174] S. Lautru and G.L. Challis, *Substrate recognition by nonribosomal peptide synthetase multi-enzymes*, Microbiol. **150**, 1629-1636 (2004).
- [175] C. Khosla, R.S. Gokhale, J.R. Jacobsen and D.E. Cane, *Tolerance and specificity of polyketide synthases*, Annu. Rev. Biochem. **68**, 219-253 (1999).
- [176] J. Grünwald and M.A. Marahiel, *Chemoenzymatic and template-directed synthesis of bioactive macrocyclic peptides*, Microbiol. Mol. Biol. Rev. **70**, 121-146 (2006).
- [177] H.v. Döhren, R. Dieckmann and M. Pavela-Vrancic, *The nonribosomal code*, Chem. Biol. **6**, R273-R279 (1999).
- [178] R. Finking and M.A. Marahiel, *Biosynthesis of nonribosomal peptides*, Annu. Rev. Microbiol. **58**, 453-488 (2004).
- [179] M.V. Volkenshtein and A.M. Eliasevich, *On the theory of mutation*, Sov. Phys. Doklady, **136**, 1216-1218 (1961).
- [180] B.K. Davis, *Entropy in template-directed polymerization*, Nature **206**, 183-184 (1965).
- [181] J.R. Arias-Gonzalez, *Entropy involved in fidelity of DNA replication*, PLoS ONE **7(8)**, e42272 (2012).

- [182] D. Andrieux and P. Gaspard, *Nonequilibrium generation of information in copolymerization processes*, Proc. Natl. Acad. Sci USA **105**, 9516-9521 (2008).
- [183] D. Andrieux and P. Gaspard, *Molecular information processing in nonequilibrium copolymerizations*, J. Chem. Phys. **130**, 014901 (2009).
- [184] A. Turing, *On computable numbers, with an application to the entscheidungs-problem*, Proc. Lond. Math. Soc. **43**, 230-265 (1936).
- [185] R.A. Mooney, I. Artsimovitch and R. Landick, *Information processing by RNA polymerase: recognition of regulatory signals during RNA chain elongation*, J. Bacteriol. **180**, 3265-3275 (1998).
- [186] H.H. Klump, *Thermodynamic description of a copolymerisation process: the link between Maxwell's demon and the drive to compile genetic information*, Trans. Roy. Soc. South Afr. **64**, 73-75 (2009).
- [187] U. Seifert, *Stochastic thermodynamics of single enzymes and molecular motors*, Eur. Phys. J. E **34**, 26 (2011).